ISSN 0915-633X

NATIONAL INSTITUTE FOR FUSION SCIENCE

A Review on Application of MHD Theory to Plasma Boundary Problems in Tokamaks

K. Itoh

(Received Jun. 12, 1992)

NIFS-163 Aug. 1992

A Review on Application of MHD Theory to Plasma Boundary Problems in Tokamaks

Kimitaka Itoh

National Institute for Fusion Science, Nagoya 464-01, Japan

This review is prepared for presentation

at 3rd International Workshop on Plasma Edge Theory

Keywords: Edge plasma, MHD equation, tokamak, transport, scrape-off layer, H-mode, edge-localized modes, ELMs, radial electric field, plasma rotation, viscosity, beta limit, ballooning mode, magnetic well, MARFE, detachment, impurity

Abstract

A survey is made on the problems of the edge plasmas, to which the analyses based on the MHD theory have been successfully applied. Also discussed are the efforts to extend the model equation to more general (and important as well) problems such as H-mode physics.

An overview is first made on the advantages of the MHD picture, and the necessary supplementary physics are examined.

Next, one- and two-dimensional models of the spatial structure of the edge plasma is discussed. The results on the stationary structure, both analytical and numerical, are reviewed: Typical example as well as the scaling law are shown.

The instabilities associated with edge plasma is next reviewed. The surface kink mode, ballooning mode, interchange mode, resistive interchange mode and thermal instability are discussed. Role of the geometry such as the location of the X-point is studied. Influences of the atomic processes, and those of the radial electric field are also discussed.

The analysis of the H-mode transition physics is finally discussed. The boundary plasma is a nonlinear media which possesses the possibility for bifurcation in which the radial electric field plays a key role. The model of the ion viscosity is also studied. Transition physics is developed. Analysis on the self-generating oscillation is shown and the relation with ELMs is discussed.

After reviewing these problems, several comments are made to what directions the study can be deepened.

Contents

Part A

A REVIEW ON APPLICATION OF MHD THEORY TO PLASMA BOUNDARY PROBLEMS IN TOKAMAKS

Kimitaka Itoh
National Institute for Fusion Science, Nagoya 464-01, Japan

[I] Introduction

The important roles of the edge plasma have been widely recognized both on the plasma confinement research and the design study of fusion reactors. The basic physics approach was compiled in Ref.[1]. Recent experimental findings, such as the H-mode[2], had a large impact in the progress in this field, as is reviewed in [3]. One of the keys is the sensitivity of the plasma response to the change of the plasma position, such as the plasma-wall distance or the directions of the ion ∇B drift and X-point location[2,3]. It is necessary to find out the key parameter which characterizes the spatial structure in modelling the edge plasma phenomena. The impact of the plasma properties on the design of future large devices is also well known. For instance, the estimation of the heat localization width and its dynamic change (such as in the large ELMs (edge localized modes)) are critical issues.

In the study of these problems, the analysis based on the magnetohydrodynamic (MHD) equation has been performed. This equation has the advantage that phenomena of various time scales, from the Alfven transit time to transport time, can be treated and that the plasma configuration is easily taken into account. In this article, we present a brief survey on the problems in edge plasmas, for which the analysis based on the fluid equations are successfully applied. We also discuss the efforts to extend the model equation to investigate more general and important problems such as H-mode physics. We finally discuss the future possible investigations.

[II] Structure of Edge Plasmas

The plasma and geometry of our analysis are shown in Fig.1. The thick dotted line indicates the separatrix. The definition of the 'edge plasma' has not been made uniquely. We here consider that the edge plasmas are consist of the plasma (1) outside of the outermost magnetic surface (i.e., scrape-off layer) and some inside of the separatrix, i.e., in the region (2) where the inhomogeneity along the field line is appreciable or (3) in which the radial gradient length depends weakly on the minor radius. (Poloidal mesh is for 2-D calculation.)

Fig.1

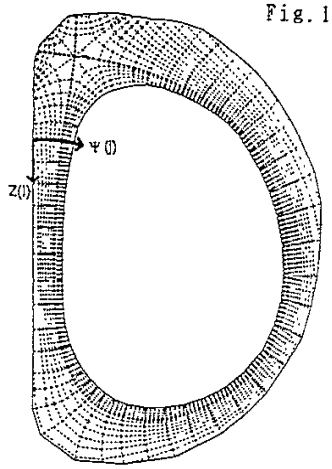

The basic equations, i.e., the continuity equations of the density, the momentum and the energy, are given in literatures as[5)]

$$\partial\rho/\partial t + \nabla\cdot(\rho\mathbf{V}) = S_n \tag{1-1}$$

$$\rho d\mathbf{V}/dt = -\nabla\cdot\mathbf{\Pi} + \mathbf{R} + \mathbf{F} + \mathbf{S}_m \tag{1-2}$$

$$\partial(\rho E_s)/\partial t + \nabla\cdot(E_s\mathbf{V}) = -\mathbf{\Pi}:\nabla\mathbf{V} + (\mathbf{R}+\mathbf{F})\cdot\mathbf{V} - \nabla\cdot\mathbf{q} + S_E \tag{1-3}$$

ρ is the mass density, E_s is the internal energy per unit mass, $\mathbf{F}$ is the external force, and other notations are standard. The MHD equations are not closed by themselves, and we need to specify the closure such as the equation of state, the stress tensor $\mathbf{\Pi}$, and the transport coefficient, and the model of the sources (S_p, $\mathbf{S}_m$, S_E).

The common choice of the closure is that the parallel transport is classical, and only the diagonal part of the stress tensor, element of which is p=nT, is kept. The frictional force R is calculated by Spitzer collision frequency. The classical values are used for the plasma resistivity η and parallel thermal conductivity. The electron energy flux q_e is given by $q_u^e + q_T^e$, and that for ion is given by q_T^i, where

$$q_u = -0.71T_e\mathbf{j}/e + (3T_e\nu_e/2e\Omega_e)\mathbf{b}\times\mathbf{j},$$

$$q_T = -\kappa_{//}\nabla_{//}T - \kappa_\perp\nabla_\perp T + (5nT/2eB)\mathbf{b}\times\nabla T.$$

ν_e is the electron collision frequency, Ω_e is the electron cyclotron frequency, $\mathbf{b}=\mathbf{B}/B$ and $\kappa=n\chi$. The perpendicular transport coefficients are considered to be anomalous, and the prescribed form is employed.

The particle source can be calculated once the neutral density is given. This term depends on the geometry strongly. The connection with the computation on neutral dynamics is discussed in [6].

The boundary conditions at the plasma-material interface are given[7)] in the form of the Bohm sheath criterion and energy transmission coefficient $\tau_{e,i}$. The current across the plasma-wall interface is often assumed to be zero. The extension to the case where the current flows across the wall (e.g., the divertor biasing) is also possible.

The plasma distribution along the field line in the scrape-off layer is first studied. When the plasma thickness is parameterized by Δ, the parallel energy conduction equation along the field line gives[8)]

$$T(\ell)^{3.5} = T_{div}^{3.5} + 7q_{//}\ell/2\kappa_0, \quad q_{//} = B_t P_{out}/B_p 2\pi\Delta R, \tag{2}$$

where ℓ is the distance along the field line from the divertor plate, $\kappa_{//} = \kappa_0 T^{2.5}$, P_{out} is the total energy outflux to SoL, a and R are the minor and major radius, and the energy deposition in the SoL plasma is neglected for the simplicity. Though very simplified, this equation reveals essential

characters of the SoL plasma.

The Bohm sheath criterion gives the plasma parameter in front of the divertor as

$$T_d = P_{out}/G\tau_t\Gamma_{out} \text{ and } n_d = \sqrt{m_i\tau_t}(B_t/B_p 2\pi\Delta R)(G\Gamma_{out})^{3/2}/\sqrt{P_{out}},$$

where $\tau_t=\tau_e+\tau_i$, G is the enhancement factor of the particle flux in SoL plasma and Γ_{out} is the particle flux out of the main plasma. T_d and n_d are essential in evaluating the performance of the divertor.

The parameter Δ is determined by the cross field energy transport. Solving the equation $\kappa_\perp \nabla_\perp T = -q_\perp (\simeq P_{out}/4\pi^2 aR)$, the estimation of Δ is obtained in [9]. If the cross field transport is given by the Bohm-like diffusion, $\chi_\perp \propto T/eB$, we have[10]

$$\Delta/a = 5\kappa_a(LB_t/\kappa_0 aB_p)^{4/11}(R/P_{out})^{3/11} \qquad (3)$$

where L is the distance between midplane and divertor along the field line and $\kappa_\perp=\kappa_a T$. The heat flux channel becomes narrower as the power increases. It is also shown that Δ does not scale to a^1. (For instance, if $P_{out} \sim a^3$, then $\Delta \sim a^{5/11}$.)

The drift heat flux ($\nabla T \times b$ term in q_T) can also affect the heat channel[11]. This term depends on the direction of B, and can be taken into account in Eq.(3) by modifying κ_a.

The numerical analysis has been performed in order to obtain the two dimensional structure of the SoL plasma[6,12-16]. These calculations can also determine the neutral particle profile, and hence the parameter G. Example is shown in Fig.2. It is shown that the dense and cold divertor plasma is established, and the neutral particles are localized nearby.

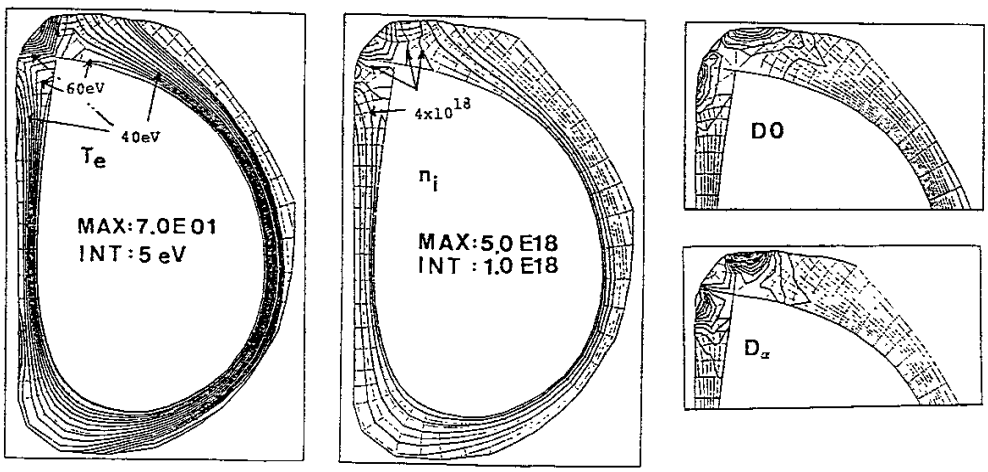

Fig.2 Examples of the 2-D simulation in the SoL region. Profiles of T_e, n_i, n_0 are given. (Model of JFT-2M plasma, the ion ∇B drift is in the direction of the X-point, the total fluxes from core are P_{out} =0.5MW and Γ_{out} =5×10^{21}/sec, respectively.)

Though the 2-D computations can now be fluently done, scaling study is desirable to have a fast grasp of the phenomena. The scaling study has been performed by using the 2-dimensional numerical code (assuming the Bohm diffusion coefficient) to give[15)]

$$n_d \sim \Gamma_{out}^{1.1} P_{out}^{0.35}, \quad T_{e,d} \sim P_{out}\Gamma_{out}^{-1}, \tag{4-1}$$

$$n_b \sim \Gamma_{out} P_{out}^{-0.3}, \quad T_{e,b} \sim P_{out}^{0.5}\Gamma_{out}^{-0.25}, \tag{4-2}$$

$$\ell_T \sim \Gamma_{out}^{0.4} P_{out}^{-0.23}, \quad \ell_n \sim \Gamma_{out}^{-0.24} P_{out}^{0.15} \tag{4-3}$$

where ℓ_T and ℓ_n are the scale lengths of the radial gradients, T/T' and n/n' ('≡d/dr), at the midplane, respectively. This result confirms that the analytic result is a good estimate. If we eliminate Γ_{out} from Eq.(4-2), we have $T_{e,b} \sim P_{out}^{0.4} n_b^{-.25}$. Equations (2) and (3) give $T_b \sim T_b^{4/11} n_b^{-2/11}$. We see that the plasma structure is well understood, and what is really necessary is the understanding of the cross field transport.

Extension to the impure plasmas has also been performed[14,16)].

[III] Stability of Edge Plasmas

MHD equation is most successfully applied to the study on the plasma stability. The strong shear associated with the separatrix and the poloidal location of the X-point are critical for the study on the stability beta limit.

The average magnetic curvature at edge of the tokamak plasma is favourable (except the case where the X-point is outside of the torus). The unstable mode may be localized in the outside of the torus (where the local bad curvature exists). The wave length along the filed line is long, i.e., $k_{//} = \mathbf{b}\cdot\nabla \simeq 1/a$ but the one across the filed line is short, $\partial/\partial\theta >> 1/a$. For the perturbation $\phi(r,\theta,\zeta)$, the ballooning transformation was introduced as [17)] $\phi(r,\theta,\zeta) = \Sigma \exp(-im\theta+n\zeta)\int_{-\infty}^{\infty} d\chi\,\phi(\chi)\exp\{i(m-nq(r))\chi\}$, where q(r) is the safety factor and m and n are the poloidal and toroidal mode numbers, respectively. (Note χ is the coordinate, not thermal conductivity. We here follow the notation of Ref.[18].) The Euler equation for high-n mode is given in a form of the ordinary differential equation.

Analytic formula for ideal MHD mode was obtained in the high aspect ratio limit of the circular plasma. The Euler equation is characterized by the three parameters, i.e., $s = rq'/q$ (local shear), $\alpha = -2Rq^2\beta^{-2}p'$ (local pressure gradient) and $\delta = (1-q^{-2})r/R$ (average well). The Euler equation is simplified as $(\partial/\partial\chi)[1+I^2]\partial\Phi/\partial\chi + \{\alpha(\cos\chi - I\sin\chi) - \delta - \tau^2(1+I^2)\}\Phi = 0$, $I = s\chi - \alpha\sin\chi$, and τ is the growth rate. The instability condition for low s case is given as $3/4[\alpha^2 - \sqrt{\alpha^4/2 - 32\alpha\delta/9}] < s < 3/4[\alpha^2 + \sqrt{\alpha^4/2 - 32\alpha\delta/9}]$, showing that the ballooning mode is stable for $\alpha < 0.8\sqrt{s}$ and $\alpha > 2.2\sqrt{s}$ (the second stability). Figure 3 illustrates the stability limit for the pressure gradient (α) as a function of the shear.

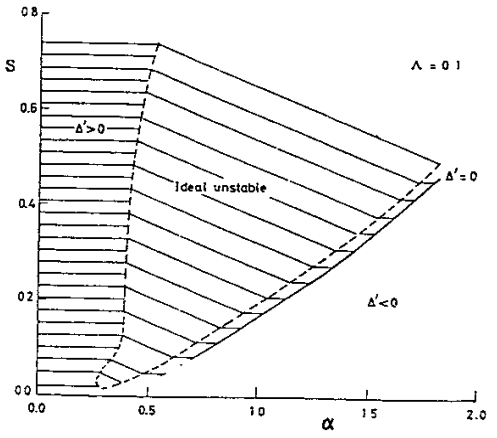

Fig. 3 Unstable region for high-n ballooning mode on the s-α plane (hatched region). Dashed line indicates the ideal stability limit. Shafranov shift is taken into account, $B_p = B_{p0}/(1-\Lambda\cos\theta)$, and $\Lambda = 0.1$. The finite resistivity widens the unstable region to low beta region. Quoted from Sykes et al.[19]

In the edge plasmas, the plasma resistivity η is small but finite. The dissipation process can destabilize the mode for the regime where ideal MHD mode is predicted to be stable. The effect of the resistivity has been studied in detail[18,19]. For the finite-resistivity plasma, Euler equation is reformed, and is characterized by the four parameters, s, α, δ and S, where S is the magnetic Raynolds number, $S = v_A \mu_0 a^2/\eta R$. For the case of the strong ballooning limit ($|s\chi| \ll 1$), the growth rate τ is determined by (growth rate τ is normalized to v_A/R)

$$\tau^3 + (k_\theta^2/2S)\tau^2 - \tau_I^2\tau - (k_\theta^2/2S)(\alpha-\delta) = 0. \qquad (5)$$

where τ_I is the growth rate in the ideal MHD limit, $\tau_I^2 = \alpha - \sqrt{\alpha/2} - \delta$. It is shown that, in the absence of well ($\delta \to 0$), the mode is unstable for all value of α, i.e., the stability beta limit is zero (see Fig. 3). The mode growth rate is given as

$$\tau \sim (\alpha k_\theta^2/2S)^{1/3} \quad \text{for } \tau_I \sim 0.$$

In the presence of the magnetic well, the critical beta for stability appear below the ideal MHD stability limit. An estimate for stability from Eq. (5) is given by $\alpha < \delta$.

The comparison study of the occurrence of the 'Type-I' ELMs[20] corresponds to the stability boundary for the ideal MHD instability, suggesting the importance of this kind of instability. However, the catastrophic nature, such that the sudden growth of the mode with $m \sim 10$ acts as the precursor of Giant ELMs[21], is not understood.

Atomic process is also the characteristic to the edge plasma, and affect the edge stability tremendously.

Global instabilities are known such as MARFE[22] and detachment. The radiation loss is modelled as $S_E = -n_e n_I L(T_e)$, where n_I is the impurity density. Models on $L(T_e)$ and the dynamic response of n_I with

respect to the perturbation are necessary to quantify the growth rate. The latter is usually denoted by the parameter $\xi=-(\tilde{n}_e/n_e+\tilde{n}_I/n_I)(T/\tilde{T})$. Asymmetric thermal instability (m=1/n=0, i.e., MARFE) can grow if[22]

$$n_I[\partial L/\partial T+\xi L/T] > \{\chi_\perp/(a-r_b)^2+\chi_{//}/q^2R^2\}, \text{ and } \xi n_I L/T > \chi_{//}/q^2R^2, \quad (6)$$

where $[r_b, a]$ is the region of the analysis, where $\partial L/\partial T$ is negative and large. If the latter condition of (6) does not hold, the poloidally symmetric mode (i.e., detachment) starts to grow. This picture is often referred to as an origin of the density limit. The lighter impurities (for which $\partial L/\partial T<0$ for the lower plasma temperature) leads to the MARFE while the heavier one to the detachment (and then disruption): These predictions are consistent with experiments.

The microscopic mode is also affected by atomic process. For instance, if the neutral density n_0 is constant, then the density fluctuation $\tilde{n}$ gives the source of fluctuation $\tilde{S}_n=\tau_n\tilde{n}\equiv n_0\tilde{n}\langle\sigma v\rangle$. This positive feed back enhances the growth rate of drift-like waves by the amount of τ_n[23]. The neutral density itself contains the fluctuating component, and a relation $\tilde{S}_n = \tau_n\tilde{n}$ is not always valid. Further analysis is required.

The sharp gradient of the radial electric field (flow velocity shear) can also affect the stability of the edge plasma. The electric field gradient influences the stability through modifying the ion orbit[24]. The effect was studied by MHD equations[25]. Stabilization is expected if

$$|E_r' k_\theta/Bk_r| \sim \tau_L \quad (7)$$

where τ_L is the linear growth rate in the absence of E_r'. Recent progress has shown that the mode amplitude is not necessarily reduced by the velocity shear, and the intensive study is under way[26]. The study in this direction was motivated by the prediction of the radial electric field at the L- and H-mode transition[27] and its confirmation by experiments[28,29].

[IV] Bifurcation Phenomena

One of the most dramatic finding in recent plasma confinement experiments was the H-mode[2]. It has shown the generic nature of the edge plasma that the multiple states are allowed for given external conditions, that the typical gradient length can be free from the minor radius, and that it has a rapid time scale for the transition. Efforts have also been made to model these phenomena in the framework of the fluid picture of the plasma, and are illustrated in the following.

A possible mechanism of the bifurcation was proposed by taking into account the effect of the loss cone[27]. The basic physics picture was that the gradient-flux relation should have the form, which is

schematically drawn in Fig.4, to explain the sequence of the transition and that this is possible at edge (not characterized by the separatrix).

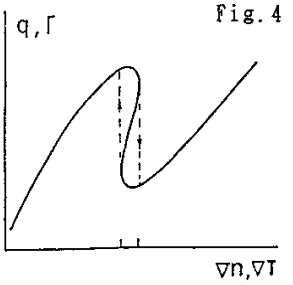

Fig.4

To quantify the model, it is necessary to study the nature of the viscosity term in the basic equation. We write the Poisson equation combining with the equation of motion as

$$\varepsilon_0\varepsilon_\perp \partial E_r/\partial t = e\{\Gamma_{re} - \Gamma_{ri} - \Gamma_{lc}\} \qquad (8)$$

where $\varepsilon_\perp$ is the perpendicular dielectric constant, Γ_{re} is the bipolar component of electron flux, Γ_{ri} is that of ion flux, and Γ_{lc} is the loss-cone current of ions. (These terms are neglected in assuming Π/p by the unit tensor.) The stationary solution is obtained by solving $\Gamma_{re}=\Gamma_{ri}+\Gamma_{lc}$. The term Γ_{lc} has the dependence on E_r as $\Gamma_{lc} \sim \rho_p n_i \nu_i \varepsilon^{-0.5}\exp\{-\Xi X^2\}$ where ν_i is the ion collision frequency, $\varepsilon=a/R$, Ξ indicates the effect of orbit squeezing due to the inhomogeneity of E_r[30], and $X=eE_r\rho_p/T$. (X is equal to the poloidal Mach number $V_pB/v_{Ti}B_p$ if $V_p=E_r/B_t$.) This shows that the loss flux can reduce if E_r is large enough. Figure 5(a) illustrates the case study that Γ_{re} is proportional to $(-n'/n+eE_r/T_e)$, and Γ_{ri} is neglected.

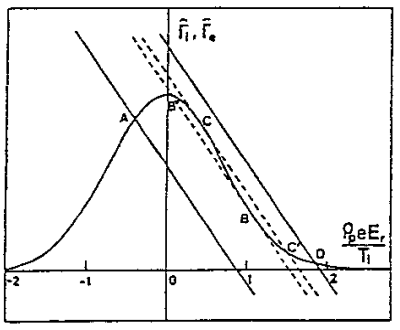

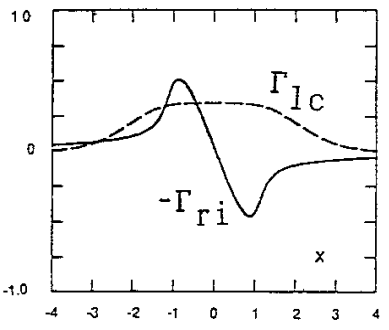

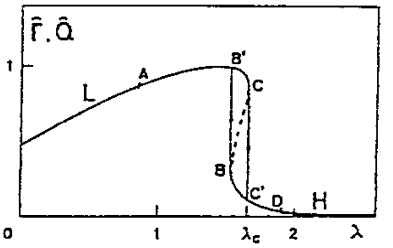

Fig.5 Balance of loss cone loss Γ_{lc} and electron loss Γ_{re} determines the radial electric field $X=e\rho_pE_r/T_i$ (a). For the case of A (small $\lambda=\rho_pn'/n$), one large-flux solution is allowed. Multiple solutions are possible for the medium λ case (B and C), and the one small-flux solution is allowed for large value of λ (D). The resultant flux as a function of λ is shown in (b). The characteristic response in Fig.4 is recovered. When the electron loss term Γ_{re} is negligible, the ion viscosity-driven flux $-\Gamma_{ri}$ and Γ_{lc} (solid and dashed lines, respectively) determine the radial electric field (c). The function $\Gamma(\lambda)$ shows the similar response as in (b).

The jump of Γ is predicted at the critical gradient

$$\lambda \equiv \rho_p n'/n = \lambda_c, \quad \text{and } \lambda_c \sim O(1) \tag{9}$$

as is shown in Fig.5(b). This example shows that the singularity of the transport property $\Gamma[\nabla n]$ can be explained by using a <u>continuous</u> function of $\Gamma[E_r]$.

The extension of the model is possible by considering Γ_{ri}[31]. The bulk viscosity generates the force on ions in the poloidal direction as $F_p \sim -m_i n_i \nu_i q^2 V_p f(X)$. The function f(X) is unity for $|X| \ll 1$ and behaves like $\exp(-X^2)$ (plateau regime) or X^{-2} (Pfirsch-Schluter regime)[31,32]. Figure 5(c) illustrates the balance of $\Gamma_{lc} = -\Gamma_{ri}$, confirming that the bifurcation can occur at the particular value of the edge gradient, $\lambda_c \sim O(1)$. Variety of the bifurcation is predicted. When the electron term Γ_{re} is negligible, the transition occurs to the more negative E_r, and that to the more positive E_r takes place if Γ_{re} is important. Other candidates such as the $\nabla\nabla V$ term or the turbulence driven flux are also studied[33].

The proposal of the electric bifurcation[27] was tested by experiments. D-III D[28] and JFT-2M[29] confirmed the radial electric field. The transition can be excited by the radial current driven by the probe and external circuit[34]. The layer width is of the order of ρ_p[29]. The nonlinear response of F_p to X is confirmed by the biasing experiment[35].

Various types of ELMs are known in experiments[22]. Some is correlated with the critical gradient of edge pressure against the ballooning mode, and some is not. The bifurcation theory predicts a model of small and continuous ELMs[36]. The hysteresis between ∇n and Γ can generates the oscillation ('limit cycle solution'). The dynamical equation (8) is solved with continuity equation and the model equation $\Gamma[X, p]$. Model equation can be formulated in the form of the Gintzburg-Landau equation as

$$\partial n/\partial t = (\partial/\partial x) D(X) \partial n/\partial x, \tag{10-1}$$

$$\upsilon \partial X/\partial t = -N(X, \lambda, n) + \mu \partial^2 X/\partial x^2 \tag{10-2}$$

where D is the effective diffusivity, $x=a-r$, υ is the smallness parameter of the order of $(\rho_i/\rho_p)^2$, μ is the shear viscosity, and N represents the current $e[\Gamma_{lc}+\Gamma_{ri}-\Gamma_{re}]$ which has the nonlinearity and depends on both E_r and ∇n. Introduction of the shear viscosity allows us to study the radial structure of the barrier. (Note that normalization is used as $x/\rho_p \to x$, $D/D_0 \to D$, $\mu/D_0 \to \mu$, $t/(\rho_p^2/D_0) \to t$, and D_0 being the diffusivity in L-phase.)

A simplified model was studied where $N(X, \lambda, n)$ is given $N(X, g)$ ($g \equiv \lambda/\nu_i$) and $N(X, g)$ is modelled by the cubic equation as in Fig.6(a). It is shown that the set equation (10) predicts the self-sustaining oscillation for a fixed value of the flux from core. This oscillation is possible in a limited area in the parameter space. Otherwise, either the high-con-

finement state (H) or low confinement state (L) is allowed. Figure 6(b) and (c) illustrate the oscillatory solution of the out flux, and the radial profile of the effective diffusivity in H and L phases. In the time-phase of good confinement, the reduction of D extends from the surface to the layer, the characteristic width of which is given $\sqrt{\mu/D}\rho_p$.

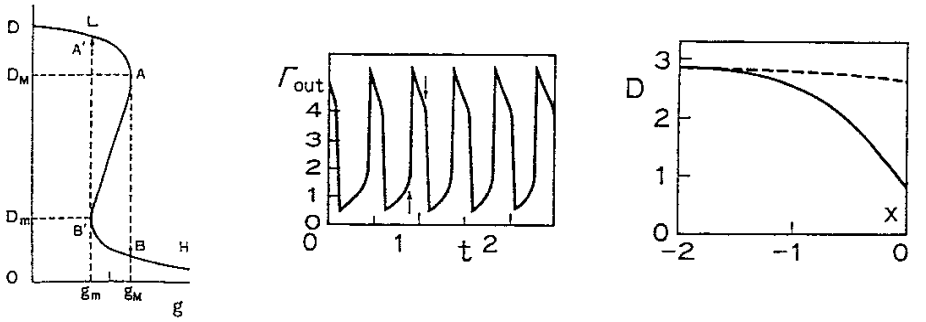

Fig.6 Model of the effective diffusivity D ($D=-\Gamma/\nabla n$) as a function of the gradient parameter λ/ν_i (a). Transition occurs at points A and B'. Two branches H and L are shown. The predicted oscillation, for given constant flux from core, is shown in (b). The profile of D at the two time slices (arrows in (b)) are shown (c). x=0 corresponds to the surface, and x<-2 to the core plasma.

These results also illustrates the importance of the viscosity in the dynamics and structure of the edge plasmas.

[V] Summary and Future Problems

In this article, we briefly surveyed the applications of the MHD theory for the understanding of the edge plasma physics. The edge phenomena is geometry-dependent, and contains various time scales. The MHD equation is a suitable tool for modelling the phenomena in the edge plasmas. It was successfully applied to study the two-dimensional profile of the plasma, the behaviour of impurities, and the stability analysis. Recent efforts has been to extend the applicable area by investigating the role of the radial electric field and the viscosity.

We here stressed that the MHD equations are not closed by themselves, and need some closure model. The study on the stress tensor Π can largely extend the area of the application. Many results are dependent on the choice of the anomalous transport coefficient.

Combining the theory that the radial inhomogeneity of E_r (or V_p) can stabilize the microscopic instabilities, the structure of the established electric field (flow velocity) are considered to suppress the microinstabilities and associated anomalous transport. The reduction of the anomalous transport further improves the confinement inside of the transport barrier. Figure 7 illustrates the present 'standard model' for the tran-

sition phenomena at edge, though many part of the elements are still qualitative yet.

There are couple of problems which require future studies. The influence of the atomic processes has been examined in the MHD analysis. Further analysis to refine models for the impurity response is required. The determination of the stability limit is now a well-defined problem for the realistic geometry and profile. There are, however, several problems; e.g., bursts of magnetic perturbation are observed and wait explanations. Taknig into account of the change of the current diffusivity due to the instability itself, the magnetic trigger phenomena has been analysed[37]. The quantitative improvement of the modelling of the viscosity and the radial currents is also necessary. The model must be extended so that the quantitative prediction of E_r is possible. Many further improvement of confinement have been proposed based on the electric bifurcation model. The verification of the model is surely an important issue.

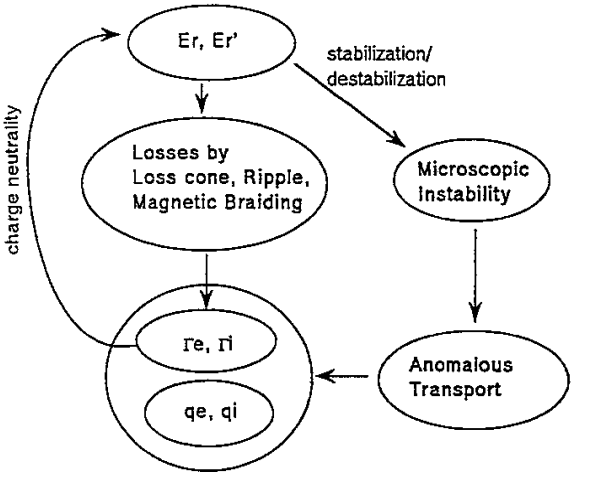

Fig. 7 Schematic diagram between the radial electric field/ rotation, the radial current, anomalous transport, and plasma fluxes.

We here have few room to show how the ***understanding*** of the edge plasma confinement is used to ***control*** it. Examples are seen[38] in the analysis of the divertor bias, or possibilities to excite the H-mode transition by the ion beam and to sustain grassy ELMs by external oscillations. The control of the edge plasma, e.g., for the good energy confinement, efficient pumping, suppression of impurities, or tolerating the heat load, is an urgent task. The understanding and modelling of edge plasma are inevitable for it, and the MHD analysis will be very useful.

Acknowledgements

The author would like to acknowledge continuous discussion and collaboration with Drs. S.-I. Itoh, N. Ueda, A. Fukuyama, and to thank Drs. M. Azumi, K. Ida, Y. Miura, H. Sanuki and K. C. Shaing for helpful discussions and supplying various data. Discussions with ASDEX group, JFT-2M group and D-III D group are also appreciated.

References

[1] *Physics of the Plasma-Wall Interactions in Controlled Fusion* (ed. D. E. Post and R. Behrisch), NATO ASI Series B131, (Prenum Press, New York, 1984).
[2] ASDEX Team: Nuclear Fusion **29** (1989) 1959.
[3] P. C. Stangeby, G. M. McCracken: Nucl. Fusion **30** (1990) 1225.
[4] F. X. Soldner, et al.: Phys. Rev. Lett. **61** (1988) 1105.
[5] K. Miyamoto: *Plasma Physics for Nuclear Fusion* (2nd Edition, Iwanami, Tokyo, 1987)
[6] N. Ueda, et al.: Nucl. Fusion **28** (1988) 1183. See also D. B. Heifetz: J. Comput. Phys. **46** (1982) 309.
[7] P. C. Stangeby: p.41 of Ref.[1] and R. Chodula: p.99 of Ref.[1]
[8] M. Keilhacker, et al.: Physica Scripta **T212** (1982) 443.
[9] F. Wagner and Lackner: p.931 of Ref.[1].
[10] K. Itoh, et al.: Nucl. Fusion **29** (1989) 1299.
[11] F. L. Hinton: Nucl. Fusion **25** (1985) 1457.
[12] J. N. Brooks,: J. Nucl. Materials **145-147** (1987) 837.
[13] B. J. Braams, et al.: in *17th EPS Conference on Controlled Fusion and Plasma Heating*, Amsterdam 1990, Part III p.1417.
[14] J. Neuhauser, et al.: Plasma Phys. Contr. Fusion **31** (1989) 1551. J. Neuhauser, et al.: Contributions to Plasma Physics **30** (1990) 95.
[15] S.-I. Itoh, et al.: Plasma Phys. Cont. Fusion **32** (1990) 415.
[16] Yu. L. Igitkhanov, et al.: in *Plasma Physics and Controlled Nuclear Fusion Research 1984* (IAEA, Vienna, 1985) Vol.2, p.113.
[17] J. W. Connor, et al.: Proc. Royal Soc. London **A365** (1979) 1.
[18] M. Azumi and M. Wakatani: Kakuyuugou Kenkyuu **66** (1991) 494.
[19] See for instance H. R. Strauss: Phys. Fluids **24** (1981) 2004, and A. Sykes, et al.: Plasma Phys. Contr. Fusion **29** (1987) 719.
[20] K. H. Burrel, et al.: in *Plasma Physics and Controlled Nuclear Fusion Research 1988* (IAEA, Vienna, 1989) Vol.1 p.193.
[21] H. Zohm, et al.: Nucl. Fusion **32** (1992) 489.
[22] J. Neuhauser, et al.: Nucl. Fusion **26** (1986) 1679.
[23] See for instance, A. S. Ware, et al.: Phys. Fluids **B4** (1992) 877.
[24] H. Sanuki: Phys. Fluids **27** (1984) 2500, S.-I. Itoh, K. Itoh: in *Plasma Physics and Controlled Nuclear Fusion Research 1988* (IAEA, Vienna, 1989) Vol.2, p.23.
[25] K. C. Shaing, et al.: in *Plasma Physics and Controlled Nuclear Fusion Research 1988* (IAEA, Vienna, 1989) Vol.2, p.13. See also H. Biglari, et al: Phys. Fluids **B2** (1989) 1.
[26] M. Wakatani, et al.: Phys. Fluids **B4** (1992) in press.
[27] S.-I. Itoh, K. Itoh: Phys. Rev. lett. **60** (1988) 2276.
[28] R. J. Groebner, et al.: Phys. Rev. Lett. **64** (1990) 3015.
[29] K. Ida, et al.: Phys. Rev. lett. **65** (1990) 1364.
[30] R. D. Hazeltine: in Bull. Am. Phys. Soc. **33** (1988) 2107.
[31] K. C. Shaing, E. C. Crume: Phys. Rev. lett. **63** (1989) 2369.
[32] T. H. Stix: Phys. Fluids **16** (1973) 1260.
[33] A. B. Hassam, et al.: in *Plasma Physics and Controlled Nuclear Fusion Research 1990* (IAEA, Vienna, 1991) Vol.2, p.311, and F. L. Hinton: Phys. Fluids **B3** (1991) 696.
[34] R. J. Taylor, et al: Phys. Rev. Lett. **63** (1989) 2365.
[35] R. R. Waynants, et al: in *Plasma Physics and Controlled Nuclear Fusion Research 1990* (IAEA, Vienna, 1991) Vol.1, p.473.
[36] S.-I. Itoh, et al.: Phys. Rev. Lett. **67** (1991) 2485.
[37] A. J. Lichtenberg, et al.: Nucl. Fusion **32** (1992) 495.
[38] Y. Miura, et al.: in *Plasma Physics and Controlled Nuclear Fusion Research 1990* (IAEA, Vienna, 1991) Vol.1 p.325, M. A. Mahdavi, et al.: ibid., p.335. T. Ohkawa, R. L. Miller: ibid., p.583. S.-I. Itoh, et al.: 'ELMy H-mode as Limit Cycle and Chaotic Oscillations in Tokamak Plasmas', NIFS-96 (NIFS, Nagoya, 1991).

Part B

Lecture Note on Application of MHD Theory to Plasma Boundary Problems in Tokamaks

[I] Introduction

Recently the important roles of the edge plasma have been widely recognized both on the plasma confinement research and the design study of fusion reactors. The basic physics approach has been compiled in Ref.[1] Recent experimental findings, such as the H-mode[2], had a large impact in the progress in this field, as is reviewed in [3]. The core plasma confinement should be more tightly coupled to the edge plasma condition than has been thought, if we judge from the phenomena like Improved Ohmic Confinement[4] (IOC), in which the reduction of the gas puffing rate leads to the peaked density profile at the core. One of the key features is the sensitivity of the plasma response to the change of the locations of the plasma, such as the plasma-wall distance or the directions of the ion ∇B drift and X-point location[2),3)]. These observations indicate the importance to take the realistic geometry (or alternatively, to find out the key parameter to characterize the spatial structure) in the modelling of the edge plasma phenomena. At the same time, various atomic processes introduce variety of the plasma dynamics in the edge region. The short mean free paths of atomic processes enhances the influence of the geometry on the global plasma structure.

Other progress of the research has been seen in evaluation of the impact of the plasma properties on the design of the plasma facing component in the future large devices. For instance, it is well known that the estimation of the heat localization width is a crucial issue. Also necessary is the evalu-

ation of the dynamic change of the heat load such as that in the large ELMs (edge localized modes). These issues also illustrate the importance of the study on the structure and dynamics of the edge plasma in a realistic plasma configurations.

In the study of these problems, the analysis based on the magnetohydrodynamic (MHD) equation has been performed. This equation has the advantage that phenomena of various time scales, from the Alfven transit time to transport time, can be treated and the realistic configuration is more easily taken into account in comparison with other approaches (such as Vlasov equation), assuming that the physics coefficient (such as transport coefficient) and boundary conditions are given.

In this article, we present a brief survey on the problems for which the analysis based on the fluid equations are successfully applied to the edge plasmas. We also discuss the efforts to extend the model equation to apply more general and important problems such as H-mode physics. We finally discuss the future possible investigations. [It is noted that the terminology of 'MHD equation' in this article is not the one for the one fluid ideal MHD equation. Various extensions to the physics processes are included in terms of the transport coefficient.]

[II] Structure of Edge Plasmas

(2.1) Fluid Equation and Boundary Condition

The plasma and geometry of our analysis are shown in Fig.1. The definition of the 'edge plasma' has not been made uniquely. We here consider that the edge plasmas are consist of the plasma (1) outside of the outermost magnetic surface (i.e., scrape-off layer) and some in the inside of the outermost magnetic surface. The latter is the plasma (2) in the region where the inhomogeneity along the field line is appreciable or (3) in the region in which the radial gradient does not scale linearly with minor radius but is determined by the distance from the surface.

The basic equations consist of the continuity equations of the density, the momentum and energy as[5)]

$$\partial\rho/\partial t + \nabla\cdot(\rho\mathbf{V}) = S_n \tag{1}$$

$$\rho d\mathbf{V}/dt = -\nabla\cdot\mathbf{\Pi} + \mathbf{R} + \mathbf{F} + \mathbf{S}_m \tag{2}$$

$$\partial(\rho E_S)/\partial t + \nabla\cdot(E_S\mathbf{V}) = -\mathbf{\Pi}:\nabla\mathbf{V} + (\mathbf{R}+\mathbf{F})\cdot\mathbf{V} - \nabla\cdot\mathbf{q} + S_E \tag{3}$$

for each plasma species (suffix to identify the species is suppressed for the simplicity), where $\mathbf{\Pi}$ is the stress tensor, $\mathbf{R}$ is the frictional force, $\mathbf{F}= q(\mathbf{E}+\mathbf{V}\times\mathbf{B})$, $E_S = V^2+w$, w is the internal energy per unit mass, S_n, $\mathbf{S}_m$, S_E are the sources of particle, momentum and energy, and other notations are conventional. One fluid MHD equations use the variables total mass density, ρ,

velocity of the plasma, $\mathbf{V}$, charge density ρ_q, and current density $\mathbf{j}$, instead of $\rho_{e,i}$ and $\mathbf{V}_{e,i}$. And the Maxwell equation is used to solve the plasma response and the field.

The MHD equations are not closed by themselves, and we need to specify the closure such as the equation of state, the stress tensor $\mathbf{\Pi}$, and the transport coefficient, and the model of the sources.

The common choice of the closure is that the parallel transport is classical, only the diagonal part of the stress tensor, element of which is $p=nT$, is kept, and E_s is approximated by $3p/2$. The frictional force $\mathbf{R}$ is calculated by Spitzer collision frequency, and interaction between neutral particles are included in S_p. The classical values are used for the plasma resistivity η and parallel thermal transport coefficient χ. The perpendicular transport coefficient are considered to be anomalous, and the prescribed form is substituted in the MHD equation.

The electron energy flux q_e is given by $q_u^e + q_T^e$, and that for ion is given by q_T^i, where

$$\mathbf{q}_u = -0.71T_e\mathbf{j}/e + (3T_e\nu_e/2e\Omega_e)\mathbf{b}\times\mathbf{j} \tag{4}$$

$$\mathbf{q}_T = -\kappa_{/\!/}\nabla_{/\!/}T - \kappa_\perp\nabla_\perp T + (5nT/2eB)\mathbf{b}\times\nabla T \tag{5}$$

ν_e is the electron collision frequency, Ω_e is the electron cyclotron frequency, $\mathbf{b}=\mathbf{B}/B$ and $\kappa=n\chi$.

The particle source can be calculated once the neutral density is given. (This term depends on the geometry strongly.

The connection with the computation on neutral dynamics is discussed in [6,7].)

The boundary conditions at the plasma-material interface are given[8,9] in the form of the Bohm sheath criterion and energy transmission coefficient $\tau_{e,i}$. The current across the plasma-wall interface is often assumed to be zero. The extension to the case where the current flows across the wall, e.g. in the study of the divertor biasing, is also possible.

In this section, we study the static (equilibrium) structure in the edge plasmas. Stability and dynamic responses are discussed in the next sections.

(2.2) Structure Along the Field Line

In studying the structure of the plasma distribution in the scrape-off layer, the competition between the parallel and perpendicular heat transports is examined. For the plasma parameter of present experiments, the energy transport along the field line is the fast process. When the plasma thickness is parameterized by Λ, the averaged temperature in the flux tube with thickness Λ is given by integrating the parallel energy conduction equation along the field line as[10]

$$T(\ell)^{3.5} = T_{div}{}^{3.5} + 7q_{//}\ell/2\kappa_0 \qquad (6)$$

where ℓ is the distance along the field line from the divertor plate, the parallel heat flux $q_{//}$ is given as

$$q_{//} = B_t P_{out} / B_p 2\pi\Delta R,$$

$$\kappa_{//} = \kappa_0 T^{2.5},$$

P_{out} is the total energy outflux to SoL, and the energy deposition in the SoL plasma is neglected for the simplicity. Though very simplified, this equation reveals essential characters of the SoL plasma.

The Bohm sheath criterion gives the plasma parameter in front of the divertor plasma as

$$T_d = P_{out} / G\gamma_t \Gamma_{out} \tag{7-1}$$

$$n_d = \sqrt{m_i \gamma_t} (B_t / B_p 2\pi\Delta R)(G\Gamma_{out})^{3/2} / \sqrt{P_{out}} \tag{7-2}$$

where

$$\gamma_t = \gamma_e + \gamma_i,$$

G is the enhancement factor of the particle flux in SoL plasma and Γ_{out} is the particle flux out of the main plasma. These parameters T_d and n_d are essential in evaluating the performance of the divertor.

(2.3) Structure Across the Field Line

The parameter Δ is determined by the cross field energy transport. The cross field transport is stronger for higher

temperature plasma, the width Δ is determined by the perpendicular diffusion near the midplane. From Eq.(6), one sees that $T \propto \ell^{2/7}$ so that $T(\ell)$ is approximated to be constant T_b near the mid plane. Solving

$$\kappa_\perp \nabla_\perp T = -q_\perp \ (\simeq P_{out}/4\pi^2 aR),$$

the estimation of Δ is obtained in [11]. If the cross field transport is given by the Bohm-like diffusion

$$\chi_\perp \propto T/eB,$$

we have[12)]

$$\Delta/a = 5\kappa_a (LB_t/\kappa_0 aB_p)^{4/11} (R/P_{out})^{3/11} \qquad (8)$$

where a and R are the minor and major radius, L is the distance between midplane and divertor along the field line and $\kappa_\perp = \kappa_a T$. The heat flux channel becomes narrower as the power increases. It is also shown that Δ does not scale to a^1. (For instance, if $P_{out} \sim a^3$, then $\Delta \sim a^{5/11}$.)

The drift heat flux ($\nabla T \times \mathbf{b}$ term in Eq.(5)) can also affect the heat channel[13)]. This term depends on the direction of $\mathbf{B}$. In the configuration like Fig.1 with B_t directed into the paper, (i.e., ∇B-drift of ions directs to the X-point), this heat flux is inward of the major radius. The heat flux across the magnetic surface reduces (outside of torus) or increased (inside of

torus). When the power is deposited mainly at the outside of the torus, this term reduces the average radial transport, reducing Δ and enhancing T_b.

(2.4) Comparison with Numerical Simulation

The numerical analysis has been performed in order to obtain the two dimensional structure of the SoL plasma[7, 14-17]. These calculations can also determine the neutral particle profile, and hence the parameter G. Example is shown in Fig.2. It is shown that the dense and cold divertor plasma is established, and the neutral particles are localized nearby.

The 2-D computations can now be fluently done, scaling study is desirable to have a fast grasp of the phenomena. The scaling study has been performed by using the 2-dimensional numerical code (assuming the Bohm diffusion coefficient) to give[16]

$$n_d \sim \Gamma_{out}^{1.1} P_{out}^{0.35}, \quad T_{e,d} \sim P_{out} \Gamma_{out}^{-1}, \tag{9-1}$$

$$n_b \sim \Gamma_{out} P_{out}^{-0.3}, \quad T_{e,b} \sim P_{out}^{0.5} \Gamma_{out}^{-0.25}, \tag{9-2}$$

$$\ell_T \sim \Gamma_{out}^{0.4} P_{out}^{-0.23}, \quad \ell_n \sim \Gamma_{out}^{-0.24} P_{out}^{0.15} \tag{9-3}$$

where ℓ_T and ℓ_n are the scale lengths of the radial gradients, T/T' and n/n', at the midplane respectively. This result confirms that the analytic result is a good estimate. If we eliminate Γ_{out} from Eq.(9-2), we have

$$T_{e,b} \sim P_{out}^{0.4} n_b^{-.25}.$$

Analytic theory [Eqs. (6) and (8)] gives

$$T_b \sim P_{out}^{4/11} n_b^{-2/11}$$

showing that the analytical estimate is confirmed by the simulation. Figure 2 also show that the electron temperature is almost constant at the plasma boundary, which is assumed in deriving Eq.(8). We see that the plasma structure is well understood, and what is really necessary is the understanding of the cross field transport.

Extension to the impure plasmas has also been performed. The screening of impurities which are generated from the divertor wall is also been analyzed quantitatively. Analytic estimates are also discussed in Refs.[18,19].

[III] Stability of Edge Plasmas

MHD equation is most successfully applied to the study on the plasma stability. The edge plasma can have a large pressure gradient (though the pressure itself is low), the study on the stability beta limit is important. Another characteristic feature of the edge plasma from the view point of the MHD stability is the strong shear associated with the separatrix, and the location of the X-point. We here briefly survey the findings of the stability analysis.

(3.1) Ballooning Mode (Ideal MHD Mode)

The average magnetic curvature at edge of the tokamak plasma is favourable, i.e., in the 'well' configuration (except the case where the X-point is outside of the torus). In such a case, the unstable mode may be localized in the outside of the torus (where the local bad curvature exists). The wave length along the filed line is long, i.e., $k_{//} = \mathbf{b}\cdot\nabla \simeq 1/a$ but the one across the filed line is short, $\partial/\partial\theta >> 1/a$. For the perturbation $\phi(r, \theta, \zeta)$, the ballooning transformation was introduced as [20]

$$\phi(r, \theta, \zeta) = \Sigma \exp(-im\theta + n\zeta) \int_{-\infty}^{\infty} d\chi \phi(\chi) \exp\{i(m - nq(r))\chi\} \qquad (10)$$

where q(r) is the safety factor and m and n are the poloidal and toroidal mode numbers, respectively. (Note χ is the coordinate, not thermal conductivity: Behaviour of $\phi(\chi)$ at $\chi \to \infty$ corresponds to that of $\phi(r)$ at the rational surface.) We here follow the

notation of Ref.[21]. The Euler equation for the ideal MHD mode is written for an ordinary differential equations for high-toroidal-mode-number modes, which has the large growth rate.

Analytic formula was obtained in the high aspect ratio limit of the circular plasma. The Euler equation is characterized by the three parameters, i.e.,

$$s = rq'/q \qquad \text{(local shear)},$$

$$\alpha = -2Rq^2B^{-2}p' \qquad \text{(local pressure gradient)}$$

and

$$\delta = (1-q^{-2})r/R \qquad \text{(average well)}$$

where $'=d/dr$. The ballooning equation is simplified as

$$(\partial/\partial\chi)[1+I^2]\partial\Phi/\partial\chi + \{\alpha(\cos\chi - I\sin\chi) - \delta - \tau^2(1+I^2)\}\Phi = 0, \qquad (11)$$

$I = s\chi - \alpha\sin\chi$, and τ is the growth rate which is normalized to v_A/R (v_A: Alfven velocity). The instability condition for low s case is given as

$$3/4[\alpha^2 - \sqrt{\alpha^4/2 - 32\alpha\delta/9}] < s < 3/4[\alpha^2 + \sqrt{\alpha^4/2 - 32\alpha\delta/9}] \qquad (12)$$

showing that the ballooning mode is stable for $\alpha < 0.8\sqrt{s}$ and $\alpha > 2.2\sqrt{s}$ (the second stability). Figure 3 illustrates the

stability limit for the pressure gradient (α) as a function of the shear.

(3.2) Effect of Plasma Dissipation on the Ballooning Mode

In the edge plasmas, the plasma resistivity η is small but finite. The dissipation process can destabilize the mode for the regime where ideal MHD mode is predicted to be stable. This process is important in estimating the beta value at the stability boundary. (The problem, whether the stability limit for beta is the experimental 'beta limit' or not, deserve further study, and discussed later.)

The effect of the resistivity has been studied in detail[22]. For the finite-resistivity plasma Eq.(11) is reformed as

$$(\partial/\partial\chi)[z/(1+zk_\theta^2/\tau S)]\partial\Phi/\partial\chi + \{\alpha(\cos\chi - I\sin\chi) - \delta - z\tau^2\}\Phi = 0, \quad (13)$$

where $z=1+I(\chi)^2$ and $k_\theta=ma/r$. The eigenvalue equation is now characterized by the four parameters, s, α, δ and S, where S is the magnetic Raynolds number,

$$S=v_A\mu_0 a^2/\eta R.$$

and v_A is the Alfven velocity. For the case of the strong ballooning limit ($|s\chi|<<1$), Eq.(13) is approximated by the Weber Equation, and the growth rate τ is determined by

$$\tau^3 + (k_\theta^2/2S)\tau^2 - \tau_I^2\tau - (k_\theta^2/2S)(\alpha-\delta) = 0. \quad (14)$$

where τ_I is the growth rate in the ideal MHD limit, $\tau_I = \alpha - \sqrt{\alpha/2} - \delta$. It is shown that, in the absence of well ($\delta \to 0$), the mode is unstable for all value of α, i.e., the stability beta limit is zero. (See Fig.4.) The mode growth rate is given as

$$\tau \sim (\alpha k_\theta^2 / 2S)^{1/3} \tag{15}$$

for the marginal stability for the ideal mode ($\tau \sim 0$). In the presence of the magnetic well, the critical beta for stability appear below the ideal MHD stability limit as shown in Fig.4(b). Simple estimate for stability from Eq.(14) is given by

$$\alpha < \delta. \tag{16}$$

The importance of the magnetic well was investigated for the JT-60 plasma (with outer X-point)[23]. Parameter D_R ($D_R = \alpha(\alpha - \delta)/s^2$) is calculated for outer-X-point configuration and limiter configuration. (The condition $D_R < 0$ is the stability criterion from the above simple estimate, Eq.(16).) Compared to the limiter case, in which D_R is negative, the outer-X-point configuration has large and positive D_R for given pressure gradient, indicating stronger instability. Experiments has also shown that the high frequency oscillations appear in the outer-X-point configuration but not in the limiter case. In this experiment, the appearance of this fluctuations coincides with the change of the sign of D_R. The influence of these oscillations on

the global confinement, however, was not analysed yet.

It is believed that the microscopic (high-n) instabilities may lead to anomalous transport with 'soft beta limit', and that the real hard 'beta limit' comes from the development of the modes with low-to-medium mode numbers. The anomalous transport based on the resistive turbulence has been developed[24], but is not enough to explain present observations.

The comparison study of the occurrence of the 'Type-I' ELMs[25] corresponds to the stability boundary for the ideal MHD instability, suggesting the importance of this kind of instability. Nonlinear simulation of the high-m pressure driven instability has recovered a rapid grow of the mode near the edge[2]. However, the catastrophic nature, such that the sudden growth of the mode with $m \sim 10$ acts as the precursor of Giant ELMs[26], is not understood.

(3.3) Instabilities Driven by Atomic Processes

Atomic process is also the characteristic to the edge plasma, and affect the edge stability tremendously.

Global instabilities are known such as MARFE[19] and detachment. The radiation loss is modeled such that

$$S_E = -n_e n_I L(T_e), \tag{17}$$

where n_I is the impurity density. Since $\partial L/\partial T_e < 0$ holds for a range of temperature and the enhanced radiation reduces the electron temperature, this loss term in principle leads to the

instability of the electron temperature. Models on $L(T_e)$ and the dynamic response of n_I with respect to the perturbation are necessary to quantify the growth rate. The latter is usually denoted by the parameter

$$\xi = -(\tilde{n}_e/n_e + \tilde{n}_I/n_I)/(\tilde{T}/T).$$

Asymmetric thermal instability (m/n=1/0, i.e., MARFE) can grow if[19]

$$n_I[\partial L/\partial T + \xi L/T] > \chi_\perp/(a-r_b)^2 + \chi_{//}/q^2R^2 \qquad (18\text{-}1)$$

($[r_b, a]$ is the region of the analysis, where $\partial L/\partial T$ is negative and large) and

$$\xi n_I L/T > \chi_{//}/q^2R^2. \qquad (18\text{-}2)$$

If Eq.(18) does not hold, the poloidally symmetric mode (m=0/n=0 mode, i.e., detachment) starts to grow.

This picture is often referred to as an origin of the density limit. If one assumes that n_I/n_e is constant, Eq.(18-1) set an upper bound for the electron edge density against the thermal instability. This theory of m=1 and m=0 modes also explains the difference of the condition for MARFE and detachment to appear. Equation (18-2) is more easily satisfied for (1) lower T_e, (2) larger device and (3) higher heating power; In other words, the lighter impurities (for which the condition

$\partial L/\partial T<0$ holds for the lower plasma temperature and Eq.(18-2) is more easily satisfied) lead to the MARFE while heavier one to the detachment (and then disruption): These prediction is consistent with experiments. The dynamics of impurities needs further analyses for quantitative comparisons.

The atomic process can also destabilize the microscopic mode such as drift wave[27]. For instance, the radiation loss increases the growth rate by the amount of $-n_I \partial L/\partial T$. If there is the constant neutral density, then the density fluctuation $\tilde{n}$ gives the source of fluctuation $\tilde{S}_n = \tau_n \tilde{n} \equiv n_0 \tilde{n} \langle \sigma v \rangle$. ($n_0$ is the neutral particle density.) This positive feed back enhances the growth rate of drift like waves by the amount of τ_n. Estimation was made that the ionization can affect the fluctuation level at edge considerably if $\tau_n > 5 \times 10^3$ (s^{-1}) for small devices. It should be noted that in this kind of computations, the density of the neutral particle is assumed to be constant (the parameter τ_n is taken as a constant parameter). This assumption in reality is not always a good model. The neutral density itself contains the fluctuating component in the case that the plasma density is fluctuating: In such a circumstance, simple relation of $\tilde{S}_n = \tau_n \tilde{n}$ ($\tau_n > 0$) is no longer valid. Further analysis is required.

(3.4) Effect of Radial Electric Field

The sharp gradient of the radial electric field is also characteristic to the boundary plasmas. It can also affect the stability of the edge plasma and gives rise to the variety of the transport properties.

The study on the stabilizing effect of E_r' was studied much in kinetic theories. The electric field gradient can influence the stability through modifying the ion orbit[28-30]. The ion Landau damping stabilizes the kinetic mode if $|E_r'/B| > |v_{Ti}\nabla n/n|$ is satisfied. Also it can change the direction of the toroidal drift of trapped particle to favourable direction.

The effect was also studied by MHD equations[31,32], in terms of the shear flow. The shear flow first tends to localize the radial extent of the mode. Stabilization is expected if

$$E_r' k_\theta / B k_r \sim \tau_L \qquad (19)$$

where τ_L is the linear growth rate in the absence of E_r'. (If the inhomogeneity of the velocity shear (d^2V/dr^2) is too large, then the Kelvin-Helmholtz instability is destabilized.) This stabilization reduces the anomalous transport which is caused by the microscopic instabilities at the edge. Recent progress has shown that the mode amplitude is not always reduced by the velocity shear[33] and the necessity to treat the electric field in a self consistent manner was pointed out. The intensive study is under way.

The study in this direction was motivated by the prediction of the radial electric field at the L- and H-mode transition[34] and its confirmation by experiments[35,36]. Also revived is the careful study of the dynamics of the radial electric field and plasma rotation. The important role of the viscosity was recognized, which is discussed in next section.

[IV] Bifurcation Phenomena

(4.1) Finding of the H-mode

One of the most dramatic finding in recent plasma confinement experiments was the H-mode[2]. This was the break through against the degradation of the energy confinement time with power. And it enlarged the possibility in achieving the ignition plasma in future devices. At the same time it has cast the physics picture that the plasma surface has the generic nature that the multiple states are allowed for given external conditions, that the spatial structure (typical gradient length) can be free from the minor radius and that it has a rapid time scale for the transition. It thus enriched the physics of the confined plasmas. Efforts have also been made to model these phenomena in the frame work of the fluid picture of the plasma, and are illustrated in the following.

(4.2) Bifurcation of the Radial Electric Field and Rotation

After the finding of the H-mode, a model was first proposed that the transport barrier would be made in the SoL[37] due to the electric field along the field line. The experimental study clarified that the barrier exists inside of the plasma surface. This model turns out incomplete, but pointed out the possible important role of the electric field on the transport in the edge plasma.

A possible mechanism of the bifurcation of the perpendicular transport was proposed by taking into account the effect of the

loss cone[34]. The basic physics picture was that the gradient-flux relation should have the form in Fig.5 to explain the sequence of the transition (i.e., very rapid reduction of the outflux at transition followed by the establishment of the pedestal in the profile) and that this is possible at edge (not characterized by the separatrix). This model in Fig.5 can be constructed by introducing a 'hidden variable' E_r. The 'edge phenomena' indicates that (1) the gradient $\partial/\partial r$ is no longer limited to the order of 1/a but can be order of 1/(a-r) [i.e., $O(1/\rho_p)$ for $(a-r) \sim \rho_p$, ρ_p being the ion poloidal gyroradius], and that the process such as loss cone can affect the global transport.

To quantify the model, it is necessary to study the nature of the viscosity term in the basic equation. We write the Poisson Equation combining with the equation of motion as

$$\varepsilon_0 \varepsilon_\perp \partial E_r/\partial t = -e\{\Gamma_{re} - \Gamma_{ri} - \Gamma_{lc}\} \tag{20}$$

where $\varepsilon_\perp$ is the perpendicular dielectric constant, Γ_{re} is the bipolar component of electron flux, Γ_{ri} is that of ion flux, and Γ_{lc} is the loss cone current of ions. These terms are neglected in assuming Π/p by the unit tensor. The stationary solution is obtained by solving $\Gamma_{re}=\Gamma_{ri}+\Gamma_{lc}$. The term Γ_{lc} has the dependence on E_r as

$$\Gamma_{lc} \sim \rho_p n_i \nu_i \varepsilon^{-0.5} \exp\{-\Xi X^2\} \tag{21}$$

where ν_i is the ion collision frequency, $\varepsilon=a/R$, Ξ indicates the effect of orbit squeezing due to the inhomogeneity of E_r[38], and

$$X=eE_r\rho_p/T.$$

(X is equal to the so called poloidal Mach number $V_pB/v_{Ti}B_p$ if $V_p=E_r/B_t$.) This shows that the loss flux can reduce if E_r is large enough.

Figure 6(a) illustrates the case study that Γ_{re} is proportional to $(-n'/n+eE_r/T_e)$ such as the ripple diffusion, as

$$\Gamma_{re} = -D_e n[n'/n+eE_r/T_e],$$

and Γ_{ri} is neglected. The jump of Γ is predicted at the critical gradient

$$\lambda \equiv \rho_p n'/n \ \lambda_c \qquad (22)$$

and λ_c is O(1) as is shown in Fig.6(b). This example shows that the singularity of the transport property $\Gamma[\nabla n]$ can be explained by using a <u>continuous</u> function of $\Gamma[E_r]$.

The extension of the model is possible by considering Γ_{ri}[39]. The bulk viscosity generates the force on ions in the poloidal direction as

$$F_p \sim -m_i n_i \nu_i q^2 f(X) V_p,$$

where the function f(X) is[39,40]

$$f(X) \simeq 1 \quad (\text{for } |X| \ll 1)$$

and behaves in the large |X| limit like

$$f(X) \propto \exp(-X^2) \quad (\text{plateau regime})$$

$$f(X) \propto X^{-2} \quad (\text{Pfirsch-Schluter regime}).$$

Taking this form of F_p, Γ_{ir} was calculated. Figure 6(c) illustrates the balance of $\Gamma_{lc} = -\Gamma_{ri}$, confirming that the bifurcation can occur at the particular value of the edge gradient, $\lambda_c \sim O(1)$ and that the edge plasma can have bistable states for a given condition[39]. Variety of the bifurcation is also predicted. When the electron term Γ_{re} is negligible, the transition occurs to the more negative E_r, and that to the mode positive E_r takes place if Γ_{re} is important. Other candidates such as the $\nabla\nabla\nabla$ term or the turbulence driven flux are also studied[41,42].

Combining the theory that the radial inhomogeneity of E_r (or V_p) can stabilize the microscopic instabilities, the structure of the established electric field (flow velocity) are considered to suppress the microinstabilities and associated anomalous transport. The reduction of the anomalous transport further improves the confinement inside of the transport barrier. Figure 7 illustrates the present 'standard model' for the transition

phenomena at edge, though many part of the elements are still qualitative yet.

(4.3) Observation of the Structure of E_r and V_p

The proposal of the electric bifurcation[34] was tested by experiments. D-III D[35] and JFT-2M[36] confirmed the establishment of the radial electric field. Also observed is that the transition can be excited by the radial current driven by the probe and external circuit[43]. The layer width is of the order of ρ_p[36]. Experiments by the electrode have confirmed the nonlinear response of the radial current to E_r[44].

These observations seem to confirm the basic physics model of the electric bifurcation. However, there still remain the mystery. Figure 8 shows the gradients near edge of the JFT-2M plasma. Peaks of $\nabla|E_r|$, ∇T and ∇n seem to exist at different positions. It looks that future progress of the theory is necessary to understand the internal structure of the transport barrier.

(4.4) Self-Sustaining Oscillation and ELMs

Various types of ELMs are known in experiments[2,25]. Some is correlated with the critical gradient of edge pressure against the ballooning mode, and some is not. In former case, the good confinement is considered to allow the edge gradient to achieve the limit imposed from the MHD stability. Small and continuous ELMs ('grassy ELMs') needs different modelling.

The bifurcation model predicts a self-sustaining oscillation

under the constant flux from the core[45]. The hysteresis between ∇n and Γ can generates the oscillation ('limit cycle solution'). The dynamical equation (20) is solved with Eq.(1) and the model equation $\Gamma[X, \nabla n]$. Simplified model equation can be formulated in the form of the Gintzburg-Landau Equation as

$$\partial n/\partial t = (\partial/\partial x)D(X)\partial n/\partial x, \tag{23-1}$$

$$\upsilon \partial X/\partial t = -N(X, \lambda, n) + \mu \partial^2 X/x^2 \tag{23-2}$$

where D is the effective diffusivity, x=a-r, υ is the smallness parameter of the order of $(\rho_i/\rho_p)^2$, μ is the shear viscosity, and N represents the current $e[\Gamma_{ic}+\Gamma_{ri}-\Gamma_{re}]$ which has the nonlinearity and depends on both E_r and ∇n. Introduction of the shear viscosity allows us to study the radial structure of the barrier. The transition may occur on one magnetic surface. The velocity V_p and field E_r cannot be discontinuous, and the transition on a magnetic surface propagates to different magnetic surface by the ion viscosity. [Note that normalization is used as

$$x/\rho_p \rightarrow x,\ D/D_0 \rightarrow D,\ \mu/D_0 \rightarrow \mu,\ t/(\rho_p{}^2/D_0) \rightarrow t$$

(D_0 being the typical diffusivity in the L-phase.)]

A simplified model was studied where $N(X, \lambda, n)$ is given $N(X, g)$ ($g \equiv \lambda/\nu_i$) and $N(X, g)$ is modeled by the cubic equation as in Fig.9(a). It is shown that the set equation (22) predicts the self-sustaining oscillation for a fixed value of the flux from

core. This oscillation (limit cycle solution) is possible in a limited area in the parameter space. Otherwise, either the high-confinement state (H) or low confinement state (L) is allowed. Figure 9(b) and (c) illustrate the oscillatory solution of the out flux, and the radial profile of the effective diffusivity in H and L phases.

In the time-phase of good confinement, the spatial structure shows that the reduction of D extends from the surface to the layer, the characteristic width of which is given $\sqrt{\mu/D}\rho_p$. The diffusion Prandtl number has an important role in determining the thickness of the transport barrier. Since the value of D(x) takes the intermediate values of D in L- and H- branches of Fig.9(a), this layer is also called as the mesophase of the two states.

These results also illustrates the importance of the viscosity in the dynamics and structure of the edge plasmas.

[V] Summary and Future Problems

In this article, we briefly survey the applications of the MHD theory for the understanding of the edge plasma physics. It is known that the edge phenomena is strongly geometry-dependent, and contains various time scales. From this point of view, the MHD equation is a suitable tool for modelling the phenomena in the edge plasmas. It was successfully applied to study the two-dimensional profile of the plasma, the behaviour of impurities, and the stability analysis. Recent efforts are to extend the applicable area by investigating the role of the radial electric field and the ion viscosity.

We here also stressed that the MHD equations are not closed by themselves, and need some closure model. It is illustrated in §IV that the study on the viscosity tensor can largely extend the area of the application. Many results are shown here to be dependent on the choice of the anomalous transport coefficient. Experimental studies on χ in the SoL are in progress as is reviewed in Ref.[3], and the improvement of our knowledge can be expected. At the same time, the research in this direction must be enforced.

The influence of the atomic processes are also examined in the MHD analysis by proper choice of the models on the radiation loss, particle source, CX loss and so on. A successful example is seen in the model of ELMs and detachment, and hence gave an insight for the density limit disruption. The analysis has also shown that not only the static radiation structure (MARFE) but also the oscillation nature of the radiation[16]. Further

analysis would be required for research in this direction with refined models for the impurity response.

One particular example is the problems in the braided magnetic field. The separatrix configuration is vulnerable to the braiding due to the error field or to the instability. The destruction of the flux surface is sometimes introduced artificially in order to control edge plasmas. The braiding at one hand causes homogeneity, but at the same time gives rise to the new structure.

The MHD stability analysis has made progress, and the determination for the stability limit is now a well-defined problem in a realistic geometry and plasma profiles. There are, however, several problems associated with the MHD instability near edge. Largest one is the problem of the trigger. Bursts of magnetic perturbation are observed, suggesting that the dramatic change of the growth rate. Figure 10 is an example form PBX-M, where a sudden growth of the fluctuations within the time of the order of 10μsec[46]. The rate of the change of τ, $\partial\tau/\partial t$, can be estimated by $(\partial\tau/\partial\beta')(\partial\beta'/\partial t)$. The typical time for the change of β is required to get a large value of τ after the parameter β' reaches the critical value for instability. This time period seems too slow compared to the rise time of bursts. A method to model the trigger problem was proposed in [47]. Another problem is the prediction of the stability boundary in the presence of the plasma dissipation, which dramatically reduce the critical value. Usual argument is that the dissipative mode only enhance the anomalous transport but the ideal mode really limits the

beta. This kind of hypothesis must be examined more carefully.

The quantitative improvement of the modelling of the viscosity and the radial currents is also necessary. It is worth to extend to the level that the quantitative prediction of E_r is possible. Some of the elements $\Gamma_{e,i}$ has been confirmed by experiments. Figure 11 is the data from TEXTOR on the radial current due to the bulk viscosity[44]. Many further improvement of confinement have been proposed based on the electric bifurcation model. The verification of the model is surely an important issue. The study on the time-dependent problems has shown that the fruitful results are expected from the MHD approach.

The research on the electric field and viscosity is also inevitable in promoting the research of the impurity-related problems. For instance, the thermal instability critically depends on the parameter $(\tilde{n}_I/n_I)/(\tilde{T}_e/T_e)$. Recently, careful experimental study on the impurity transport was made on ASDEX[48], and it was found that the anomalous transport affects considerably the impurity flux. It is also known that the difference of wall material can lead the dramatic difference of the plasma response. Examples are found in the super H-mode for Boronized wall (D-III D), change of the current quench time at disruption between carbonized wall and Beryllium wall, so on. Intensive research is required in future.

It is also noted that the study on the edge barrier is the problem of the self-generating structure across the field. It is well known that there is a self-generating structure along the

field line, such as the double layer, the width of which is independent of the system size. The barrier of the H-mode would be the first example that the cross-field gradient is free from the system size and reaches its new characteristic length. (The bifurcation model predicts the length scale with $\sqrt{\mu/D}\rho_p$.) It may reveal the generic nature of the confined plasma and have a future impact to wider area of the physics.

These studies may lead to the understanding of the more mysterious nature of the plasma. For instance, the core plasma profile can be peaked when the edge neutral density changes through affecting the radial electric field profile[49] (model of IOC[4]). The interaction between the core and edge plasma has not been clarified enough.

We here have few room to show how the understanding of the edge plasma confinement is used to control it. One example is seen in the analysis of the divertor bias[50,51]. The other is the excitation of the H-mode transition by the ion beam[52], or the sustenance of grassy ELMs by external oscillations[53]. The control of the edge plasma, e.g., for the good energy confinement, efficient pumping, suppression of impurities, or tolerating the heat load, are urgent tasks. The proper modelling of edge plasma is inevitable for it, and the MHD analysis will still be very useful in the research in this direction.

Acknowledgements

It is a great pleasure to acknowledge continuous discussion and collaboration with Drs. S.-I. Itoh, N. Ueda, A. Fukuyama. The author would like to thank Drs. M. Azumi, K. Ida, Y. Miura, H. Sanuki and K. C. Shaing for helpful discussions and supplying various data. Discussions with ASDEX group, JFT-2M group and D-III D group is also appreciated. This work is partly supported by the Grant-in-Aid for Scientific Research of Ministry of Education of Japan.

References

[1] *Physics of the Plasma-Wall Interactions in Controlled Fusion* (ed. D. E. Post and R. Behrisch), NATO ASI Series B131, (Prenum Press, London/New York, 1984).

[2] ASDEX Team: Nuclear Fusion **29** (1989) 1959.

[3] P. C. Stangeby, G. M. McCracken: Nucl. Fusion **30** (1990) 1225.

[4] F. X. Soldner, et al.: Phys. Rev. Lett. **61** (1988) 1105.

[5] K. Miyamoto: *Plasma Physics for Nuclear Fusion* (2nd Edition, Iwanami, Tokyo, 1987)

[6] D. B. Heifetz: J. Comput. Phys. **46** (1982) 309. See also M. Petravic, et al.: in *Plasma Physics and Controlled Nuclear Fusion Research 1984* (IAEA, Vienna, 1985) Vol.2, 103.

[7] N. Ueda, et al.: Nucl. Fusion **28** (1988) 1183.

[8] See for instance P. C. Stangeby: p.41 of Ref.[1] and

[9] R. Chodula: p.99 of Ref.[1]

[10] M. Keilhacker, et al.: Physica Scripta **T212** (1982) 443.

[11] F. Wagner and Lackner: p.931 of Ref.[1].

[12] K. Itoh, et al.: Nucl. Fusion **29** (1989) 1299.

[13] F. L. Hinton: Nucl. Fusion **25** (1985) 1457.

[14] J. N. Brooks,: J. Nucl. Materials **145-147** (1987) 837.

[15] J. Neuhauser, et al.: Plasma Phys. Contr. Fusion **31** (1989) 1551, and
J. Neuhauser, et al.: Contributions to Plasma Physics **30** (1990) 95.

[16] S.-I. Itoh, et al.: Plasma Phys. Cont. Fusion **32** (1990) 415.

[17] B. J. Braams, et al.: *Proc. 17th EPS Conference on*

Controlled Fusion and Plasma Heating, Amsterdam 1990, Part III, 1417.

[18] Yu. L. Igitkhanov, et al.: in *Plasma Physics and Controlled Nuclear Fusion Research 1984* (IAEA, Vienna, 1985) Vol.2, 113.

[19] J. Neuhauser, et al.: Nucl. Fusion **26** (1986) 1679.
See also T. E. Stringer: *Proc. 12th EPS Conference on Controlled Fusion and Plasma Physics*, Budapest 1985, Part I, p86.

[20] J. W. Connor, et al.: Proc. Royal Soc. London **A365** (1979) 1.

[21] A survey is made by M. Azumi and M. Wakatani: Kakuyuugou Kenkyuu **66** (1991) 494 (in Japanese).

[22] See for instance H. R. Strauss: Phys. Fluids **24** (1981) 2004, A. Sykes, et al.: Plasma Phys. Contr. Fusion **29** (1987) 719, and C. M. Bishop, Nucl. Fusion **26** (1986) 1063.

[23] M. Azumi: private communications (1991)
See also JT-60 Group: *Plasma Physics and Controlled Nuclear Fusion Research 1988* (IAEA, Vienna, 1989) Vol.1 p.111.

[24] B. A. Carreras, et al.: Phys. Rev. Lett. **50** (1983) 503.

[25] K. H. Burrel, et al.: in *Plasma Physics and Controlled Nuclear Fusion Research 1988* (IAEA, Vienna, 1989) Vol.1 p.193.

[26] H. Zohm, et al.: Nucl. Fusion **32** (1992) 489.

[27] For recent studies, see for instance, A. S. Ware, et al.: Phys. Fluids **B4** (1992) 877.

[28] H. Sanuki: Phys. Fluids **27** (1984) 2500, see also A. El-Nadi, H. Hassan: Phys. Fluids **25** (1982) 2140.

[29] S.-I. Itoh, K. Itoh: in *Plasma Physics and Controlled Nuclear Fusion Research 1988* (IAEA, Vienna, 1989) Vol.2, p23

[30] S.-I. Itoh, et al.: J. Phys. Soc. Jpn. **60** (1991) 2505.

[31] K. C. Shaing, et al.: in *Plasma Physics and Controlled Nuclear Fusion Research 1988* (IAEA, Vienna, 1989) Vol.2, p13.

[32] H. Biglari, et al: Phys. Fluids **B2** (1989) 1.

[33] M. Wakatani, et al.: Phys. Fluids **B4** (1992) in press.

[34] S.-I. Itoh, K. Itoh: Phys. Rev. lett. **60** (1988) 2276.

[35] R. J. Groebner, et al.: Phys. Rev. Lett. **64** (1990) 3015.

[36] K. Ida, et al.: Phys. Rev. lett. **65** (1990) 1364.

[37] T. Ohkawa, F. L. Hinton: Phys. Rev. Lett. **51** (1983) 2101.

[38] R. D. Hazeltine: in Bull. Am. Phys. Soc. **33** (1988) 2107.

[39] K. C. Shaing, E. C. Crume: Phys. Rev. lett. **63** (1989) 2369.

[40] T. H. Stix: Phys. Fluids **16** (1973) 1260.

[41] A. B. Hassam, et al.: in *Plasma Physics and Controlled Nuclear Fusion Research 1990* (IAEA, Vienna, 1991) Vol.2, 311, and

[42] F. L. Hinton: Phys. Fluids **B3** (1991) 696.

[43] R. J. Taylor, et al: Phys. Rev. Lett. **63** (1989) 2365.

[44] R. R. Weynants, D. Bora, T. Delvigne, et al.: in *Plasma Physics and Controlled Nuclear Fusion Research 1990* (IAEA, Vienna, 1991) Vol.1, 473.

[45] S.-I. Itoh, et al.: Phys. Rev. Lett. **67** (1991) 2485.

[46] S. M. Kaye, et al.: Nucl. Fusion **30** (1990) 2621

[47] A. J. Lichtenberg, et al.: Nucl. Fusion **32** (1992) 495.

[48] G. Fussmann, et al.: Plasma Phys. Contr. Fusion **33** (1991)

1677.

[49] S.-I. Itoh: J. Phys. Soc. Jpn. **59** (1990) 3431.

[50] Y. Miura, et al.: *Plasma Physics and Controlled Nuclear Fusion Research 1990* (IAEA, Vienna, 1991) Vol.1, p325.

[51] M. A. Mahdavi, et al.: *Plasma Physics and Controlled Nuclear Fusion Research 1990* (IAEA, Vienna, 1991) Vol.1, p335.

[52] T. Ohkawa, R. L. Miller: *Plasma Physics and Controlled Nuclear Fusion Research 1990* (IAEA, Vienna, 1991) Vol.1, p583.

[53] S.-I. Itoh, et al.: 'ELMy H-mode as Limit Cycle and Chaotic Oscillations in Tokamak Plasmas' NIFS-Report 96 (NIFS, Nagoya, 1991)

Figure captions

Fig. 1 Example of the edge plasma region (model of JFT-2M plasma). Thick dashed line denotes the separatrix magnetic surface, in which the magnetic surfaces (shown by thin dotted lines) are nested and closed. Out of the separatrix, field lines are connected to the divertor region or the wall. Meshes in the poloidal direction are given for the two-dimensional computations. Flux surfaces of the core plasma are not drawn.

Fig. 2 Examples of the plasma and neutral profiles in the SoL region. Profiles of T_e, n_i, n_0, and D_α are given. (Model of JFT-2M plasma, the ion ∇B direction is into the X-point, the total fluxes from core are P_{out} =0.5MW and Γ_{out} = 5×10^{21}/sec, respectively.) (Quoted from Ref.[16].)

Fig. 3 Stability-instability boundary for the ideal MHD mode in the s-α plane. (Quoted from Ref.[21].)

Fig. 4 Stability-instability boundary in the s-α plane for the resistive plasma (a). The effect of the Shafranov shift (B_p =$B_{p0}/(1-\Lambda\cos\theta)$) is taken into account, which stabilizes the resistive mode in the second stability region. The finite resistivity extends the unstable region to low beta region. [There is a narrow stable region near α=0 in case δ is not zero.] (Quoted from Sykes et al., [22].)

Example of the growth rate is shown in (b) in the presence of magnetic well. The critical beta-limit for the resistive instability is smaller than the prediction of ideal MHD theory. The case of $S=10^4$ is shown. (Quoted from Strauss, [22].)

Fig.5 Schematic model relation of the gradient (∇n, ∇T) and flux (Γ, q) for the edge plasma, in order to explain the rapid change of the energy loss at the onset of H-mode transition (a). Singularities appear at particular values of the gradient. The gradient-flux relation for the case of the slow transition is shown in (b) for the reference.

Fig.6 Balance of the loss cone loss Γ_{lc} and electron loss Γ_{re} determines the radial electric field $X=e\rho_p E_r/T_i$ (a). For the case of A (small $\lambda=\rho_p n'/n$), one large-flux solution is allowed. Multiple solutions are possible for the medium λ case (B and C), and the one small-flux solution is allowed for large value of λ (D). The resultant flux, as a function of λ, is shown in (b). The characteristic response in Fig.5 is recovered. When the electron loss term Γ_{re} is negligible, the ion viscosity-driven flux Γ_{ri} and Γ_{lc} determine the radial electric field (c). The function $\Gamma(\lambda)$ shows the similar response as in (b).

Fig.7 Schematic diagram between the radial electric field/ rotation, the radial current, anomalous transport, and

plasma fluxes.

Fig. 8 Profile of the gradients of the radial electric field (a), temperature (b), and density (c) for the H- and L-mode in the JFT-2M plasma. Solid lines indicate the result in the H-mode, and dashed lines are for the L-mode.

Fig. 9 Model of the effective diffusivity D ($D=-\Gamma/\nabla n$) as a function of the gradient parameter $g \equiv \lambda/\nu_i$ (a). Transition occurs at points A and B'. Two branches, H and L, are shown. The intermediate branch (between A and B') are the thermodynamically unstable branch. The predicted oscillation, for given constant flux from core, is shown in (b). The radial shape of D at the two time slices (high- and low-confinement states) are shown in (c).

Fig. 10 Burst of the magnetic fluctuation was observed prior to the giant ELM in the PBX-M. This burst of fluctuation precedes to the occurrence of the ELM. The rise time of the fluctuation is of the order of 10μsec. (Quoted from [46].)

Fig. 11 Radial current driven by the bulk viscosity was studied in TEXTOR. (Quoted from [44].)

Fig. 1

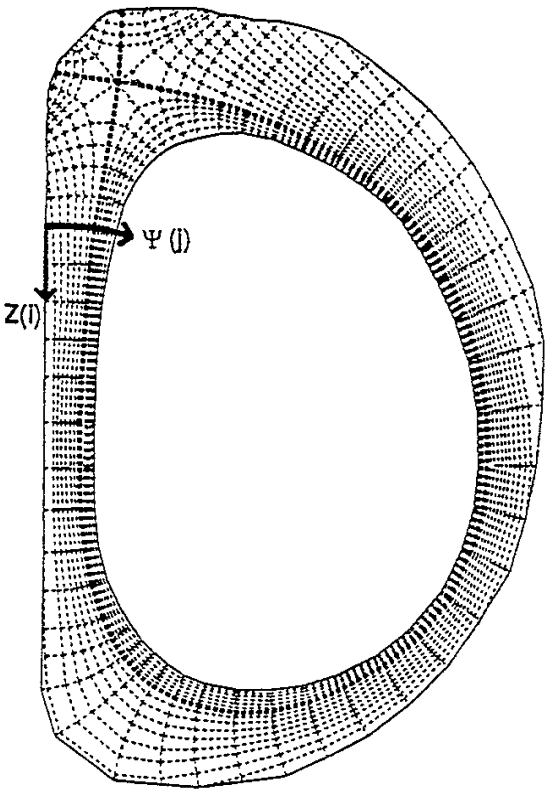

Fig. 2

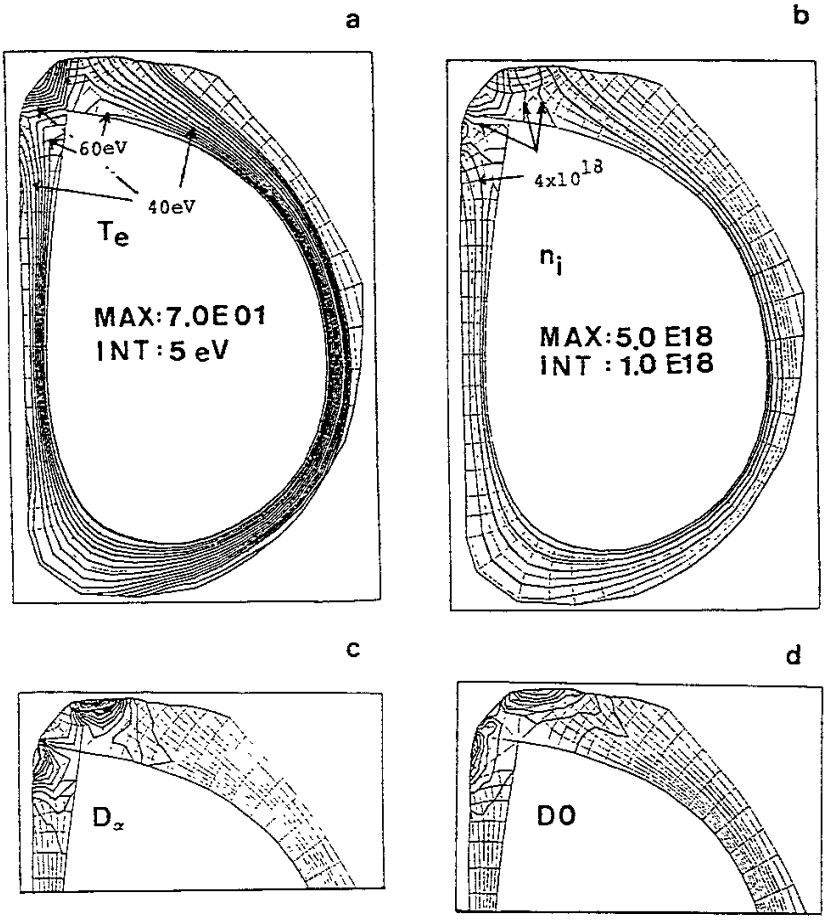
a
60eV
40eV
T_e
MAX:7.0E01
INT:5 eV
b
$4x10^{18}$
n_i
MAX:5.0 E18
INT : 1.0 E18
c
D_α
d
DO

Fig. 3

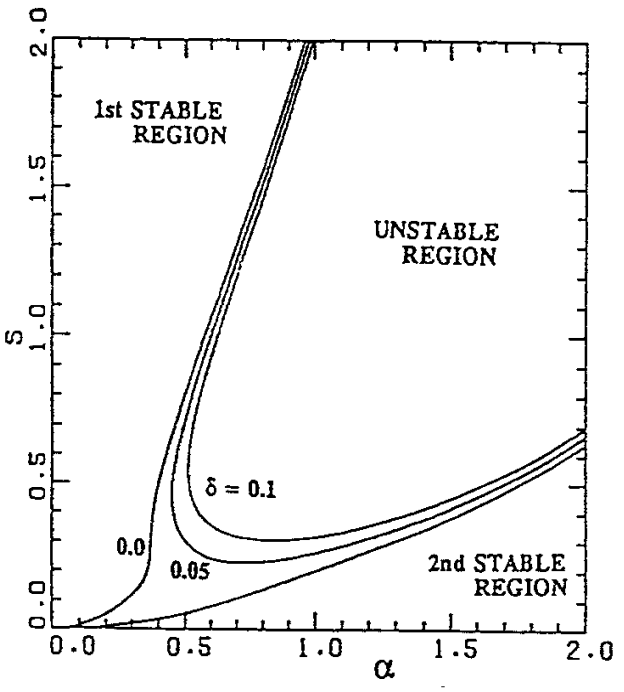
1st STABLE
REGION
UNSTABLE
REGION
δ = 0.1
0.0
0.05
2nd STABLE
REGION
S
α
0.0
0.5
1.0
1.5
2.0

Fig. 4

(a)

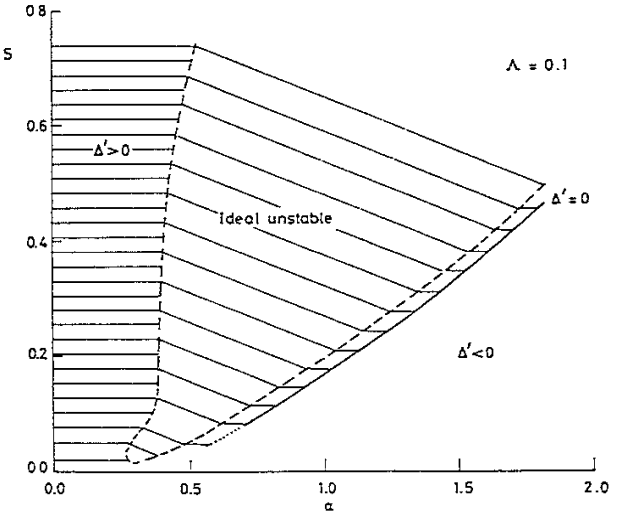
S
0.8
0.6
0.4
0.2
0.0
0.0
0.5
1.0
1.5
2.0
α
Λ = 0.1
Δ'>0
Ideal unstable
Δ'=0
Δ'<0

(b)

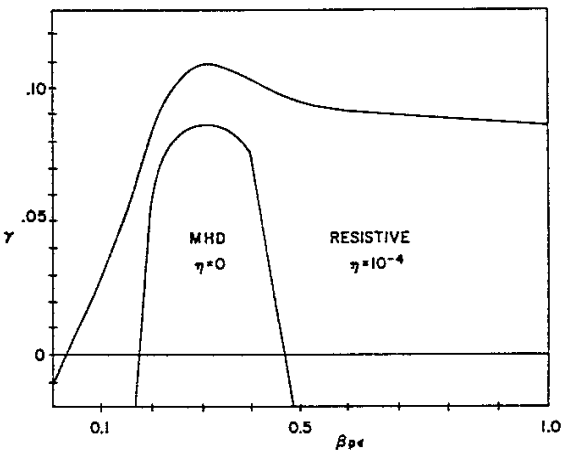
.10
.05
0
γ
MHD
η=0
RESISTIVE
η=10⁻⁴
0.1
0.5
1.0
βpα

Fig. 5

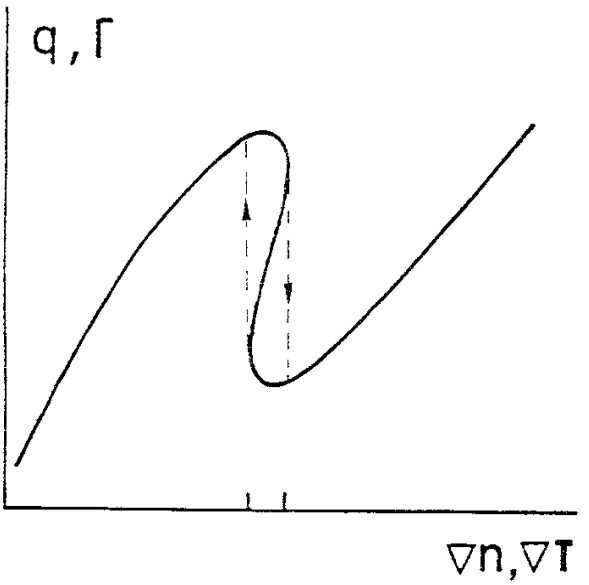

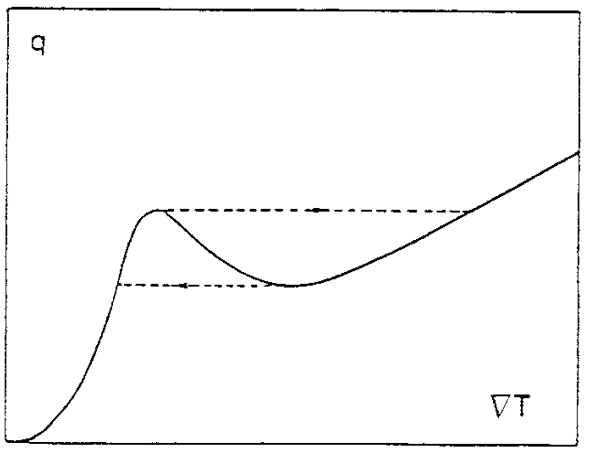

Fig. 6

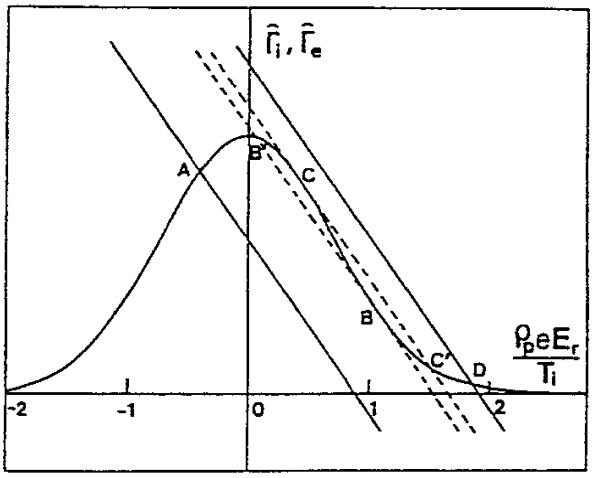
$\hat{\Gamma}_i, \hat{\Gamma}_e$
A
B'
C
B
C'
D
$\frac{\rho_{pe} E_r}{T_i}$
-2
-1
0
1
2

(a)

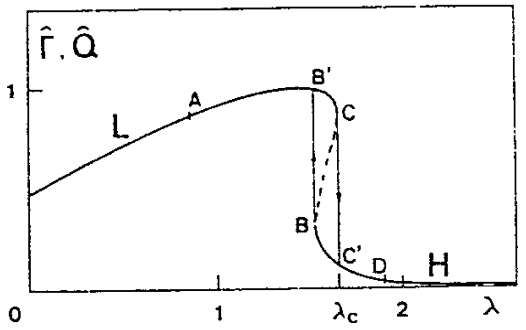
$\hat{\Gamma}, \hat{Q}$
1
L
A
B'
C
B
C'
D
H
0
1
λ_c
2
λ

(b)

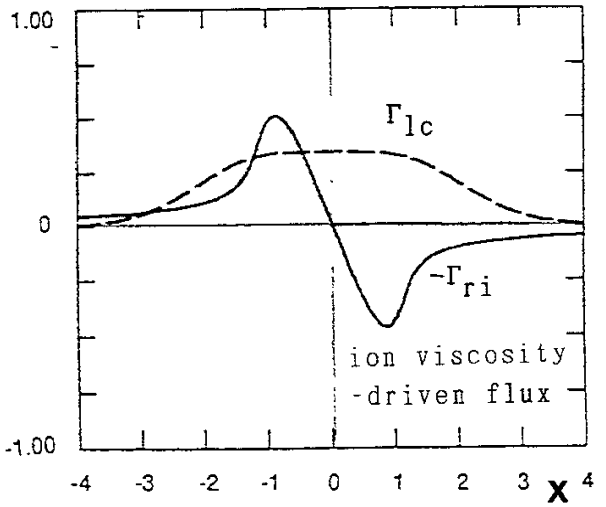
1.00
0
-1.00
Γ_{lc}
$-\Gamma_{ri}$
ion viscosity
-driven flux
-4
-3
-2
-1
0
1
2
3
4
X

(c)

Fig. 7

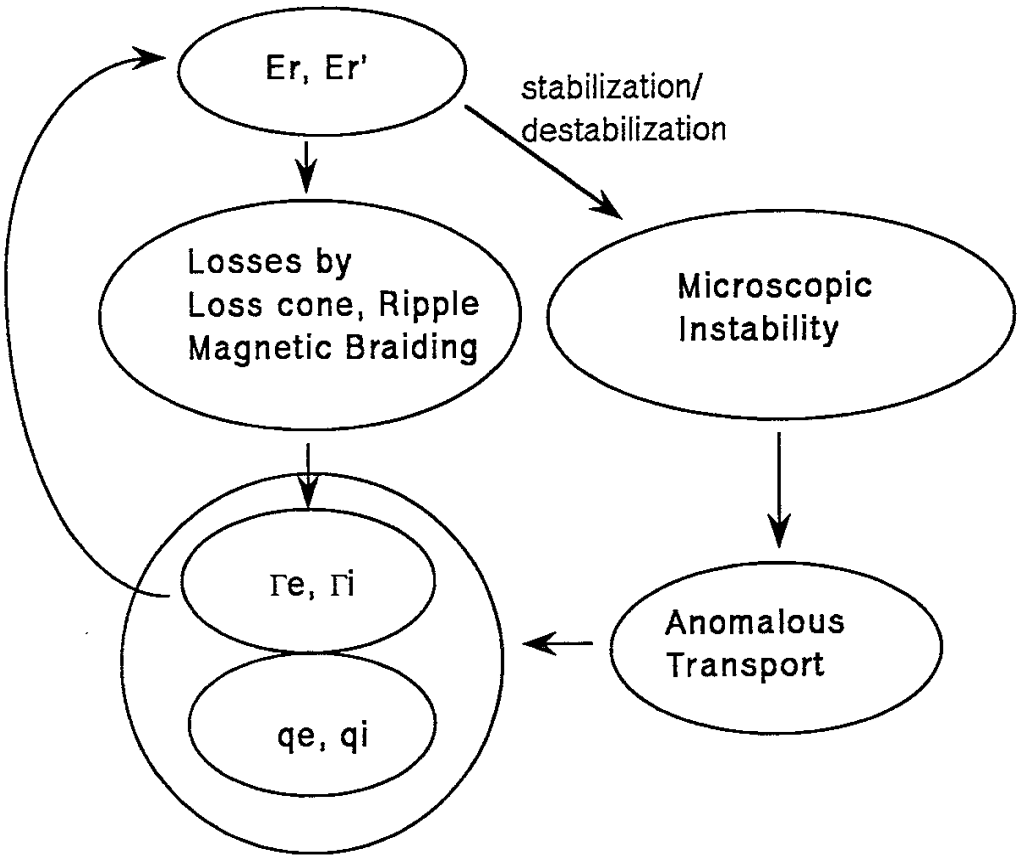
Er, Er'
stabilization/
destabilization
Losses by
Loss cone, Ripple
Magnetic Braiding
Microscopic
Instability
Γe, Γi
qe, qi
Anomalous
Transport

Fig. 8

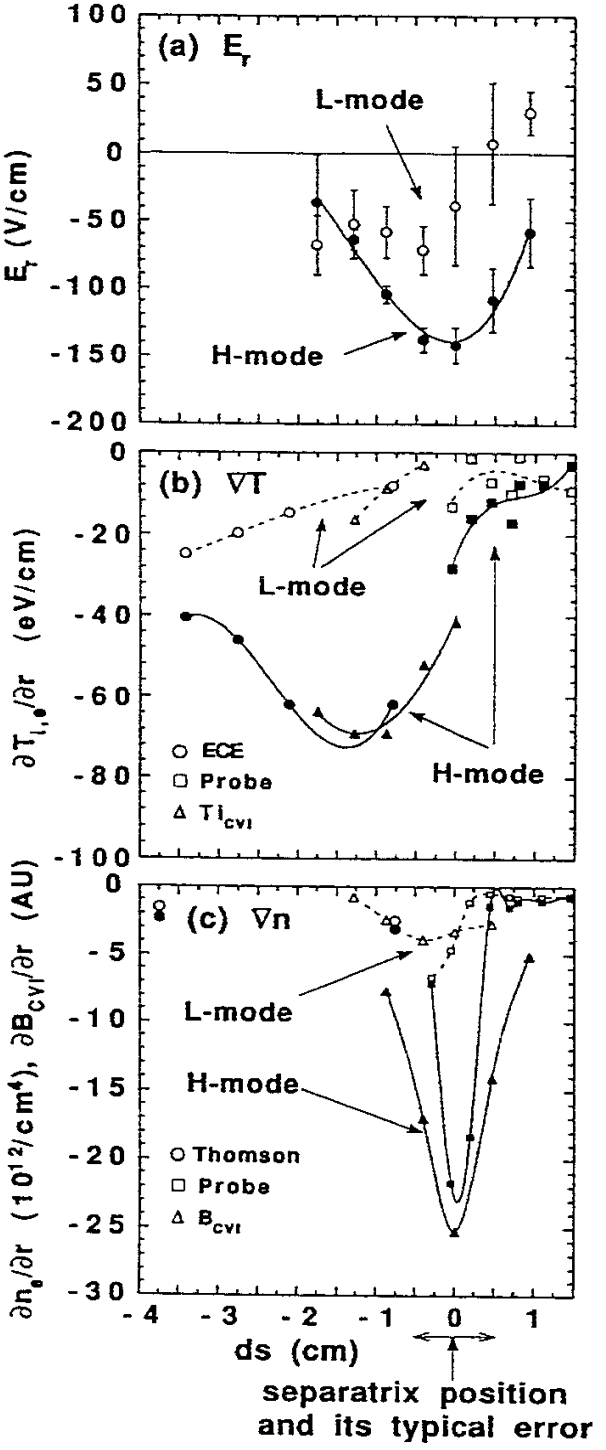
(a) E_r
L-mode
H-mode
E_r (V/cm)
(b) ∇T
L-mode
H-mode
ECE
Probe
Ti_{cvi}
$\partial T_{i,e}/\partial r$ (eV/cm)
(c) ∇n
L-mode
H-mode
Thomson
Probe
B_{cvi}
$\partial n_e/\partial r$ (10^{12}/cm^4), $\partial B_{cvi}/\partial r$ (AU)
ds (cm)
separatrix position
and its typical error

Fig. 9

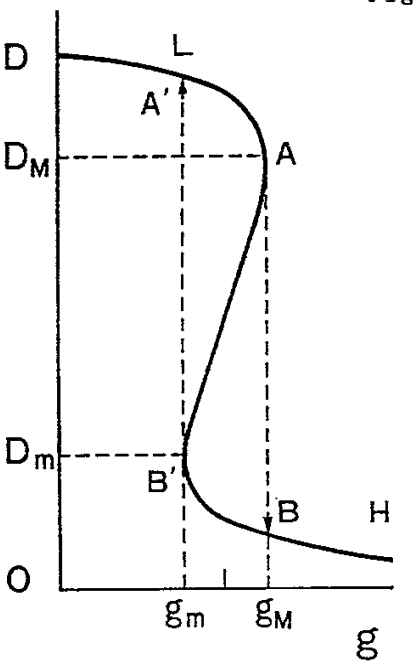

(a)

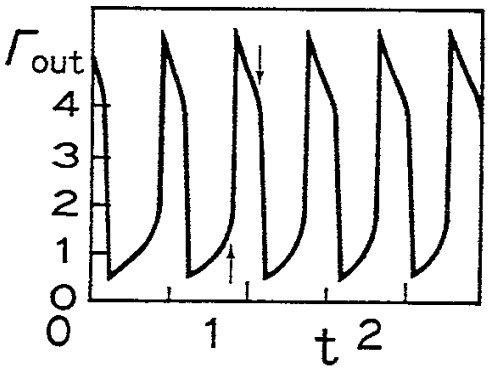

(b)

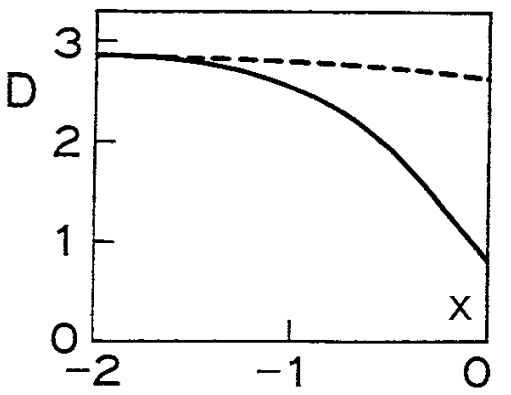

(c)

Fig.10

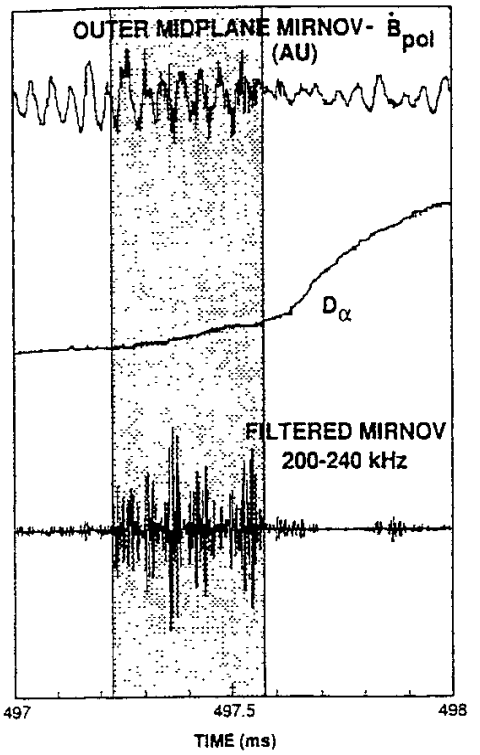
OUTER MIDPLANE MIRNOV- $\dot{B}_{pol}$ (AU)
D_α
FILTERED MIRNOV 200-240 kHz
497
497.5
498
TIME (ms)

Fig. 11

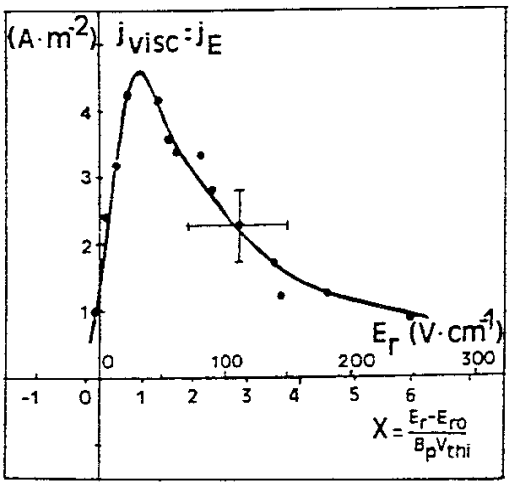
(A·m-2) jvisc : jE
4
3
2
1
Er (V·cm-1)
0
100
200
300
-1
0
1
2
3
4
5
6
X = Er-Ero / BpVthi

Recent Issues of NIFS Series

NIFS-112 M. Sasao, Y. Okabe, A. Fujisawa, H. Iguchi, J. Fujita, H. Yamaoka and M. Wada, *Development of Negative Heavy Ion Sources for Plasma Potential Measurement* ; Oct. 1991

NIFS-113 S. Kawata and H. Nakashima, *Tritium Content of a DT Pellet in Inertial Confinement Fusion* ; Oct. 1991

NIFS-114 M. Okamoto, N. Nakajima and H. Sugama, *Plasma Parameter Estimations for the Large Helical Device Based on the Gyro-Reduced Bohm Scaling* ; Oct. 1991

NIFS-115 Y. Okabe, *Study of Au^- Production in a Plasma-Sputter Type Negative Ion Source* ; Oct. 1991

NIFS-116 M. Sakamoto, K. N. Sato, Y. Ogawa, K. Kawahata, S. Hirokura, S. Okajima, K. Adati, Y. Hamada, S. Hidekuma, K. Ida, Y. Kawasumi, M. Kojima, K. Masai, S. Morita, H. Takahashi, Y. Taniguchi, K. Toi and T. Tsuzuki, *Fast Cooling Phenomena with Ice Pellet Injection in the JIPP T-IIU Tokamak;* Oct. 1991

NIFS-117 K. Itoh, H. Sanuki and S. -I. Itoh, *Fast Ion Loss and Radial Electric Field in Wendelstein VII-Λ Stellarator*; Oct. 1991

NIFS-118 Y. Kondoh and Y. Hosaka, *Kernel Optimum Nearly-analytical Discretization (KOND) Method Applied to Parabolic Equations <<KOND-P Scheme>>;* Nov. 1991

NIFS-119 T. Yabe and T. Ishikawa, *Two- and Three-Dimensional Simulation Code for Radiation-Hydrodynamics in ICF*; Nov. 1991

NIFS-120 S. Kawata, M. Shiromoto and T. Teramoto, *Density-Carrying Particle Method for Fluid* ; Nov. 1991

NIFS-121 T. Ishikawa, P. Y. Wang, K. Wakui and T. Yabe, *A Method for the High-speed Generation of Random Numbers with Arbitrary Distributions;* Nov. 1991

NIFS-122 K. Yamazaki, H. Kaneko, Y. Taniguchi, O. Motojima and LHD Design Group, *Status of LHD Control System Design ; Dec. 1991*

NIFS-123 Y. Kondoh, *Relaxed State of Energy in Incompressible Fluid and Incompressible MHD Fluid* ; Dec. 1991

NIFS-124 K. Ida, S. Hidekuma, M. Kojima, Y. Miura, S. Tsuji, K. Hoshino, M. Mori, N. Suzuki, T. Yamauchi and JFT-2M Group, *Edge Poloidal Rotation Profiles of H-Mode Plasmas in the JFT-2M Tokamak ;* Dec. 1991

NIFS-125 H. Sugama and M. Wakatani, *Statistical Analysis of Anomalous Transport in Resistive Interchange Turbulence* ;Dec. 1991

NIFS-126 K. Narihara, *A Steady State Tokamak Operation by Use of Magnetic Monopoles* ; Dec. 1991

NIFS-127 K. Itoh, S. -I. Itoh and A. Fukuyama, *Energy Transport in the Steady State Plasma Sustained by DC Helicity Current Drive* ;Jan. 1992

NIFS-128 Y. Hamada, Y. Kawasumi, K. Masai, H. Iguchi, A. Fujisawa, JIPP T-IIU Group and Y. Abe, *New Hight Voltage Parallel Plate Analyzer* ; Jan. 1992

NIFS-129 K. Ida and T. Kato, *Line-Emission Cross Sections for the Charge-exchange Reaction between Fully Stripped Carbon and Atomic Hydrogen in Tokamak Plasma*; Jan. 1992

NIFS-130 T. Hayashi, A. Takei and T. Sato, *Magnetic Surface Breaking in 3D MHD Equilibria of l=2 Heliotron* ; Jan. 1992

NIFS-131 K. Itoh, K. Ichiguchi and S. -I. Itoh, *Beta Limit of Resistive Plasma in Torsatron/Heliotron* ; Feb. 1992

NIFS-132 K. Sato and F. Miyawaki, *Formation of Presheath and Current-Free Double Layer in a Two-Electron-Temperature Plasma* ; Feb. 1992

NIFS-133 T. Maruyama and S. Kawata, *Superposed-Laser Electron Acceleration* Feb. 1992

NIFS-134 Y. Miura, F. Okano, N. Suzuki, M. Mori, K. Hoshino, H. Maeda, T. Takizuka, JFT-2M Group, S.-I. Itoh and K. Itoh, *Rapid Change of Hydrogen Neutral Energy Distribution at L/H-Transition in JFT-2M H-mode ;* Feb. 1992

NIFS-135 H. Ji, H. Toyama, A. Fujisawa, S. Shinohara and K. Miyamoto *Fluctuation and Edge Current Sustainment in a Reversed-Field-Pinch;* Feb. 1992

NIFS-136 K. Sato and F. Miyawaki, *Heat Flow of a Two-Electron-Temperature Plasma through the Sheath in the Presence of Electron Emission;* Mar. 1992

NIFS-137 T. Hayashi, U. Schwenn and E. Strumberger, *Field Line Diversion*

Properties of Finite ß Helias Equilibria; Mar. 1992

NIFS-138 T. Yamagishi, *Kinetic Approach to Long Wave Length Modes in Rotating Plasmas*; Mar. 1992

NIFS-139 K. Watanabe, N. Nakajima, M. Okamoto, Y. Nakamura and M. Wakatani, *Three-dimensional MHD Equilibrium in the Presence of Bootstrap Current for Large Helical Device (LHD)*; Mar. 1992

NIFS-140 K. Itoh, S. -I. Itoh and A. Fukuyama, *Theory of Anomalous Transport in Toroidal Helical Plasmas;* Mar. 1992

NIFS-141 Y. Kondoh, *Internal Structures of Self-Organized Relaxed States and Self-Similar Decay Phase;* Mar. 1992

NIFS-142 U. Furukane, K. Sato, K. Takiyama and T. Oda, *Recombining Processes in a Cooling Plasma by Mixing of Initially Heated Gas*; Mar. 1992

NIFS-143 Y. Hamada, K. Masai, Y. Kawasumi, H. Iguchi, A. Fijisawa and JIPP T-IIU Group, *New Method of Error Elimination in Potential Profile Measurement of Tokamak Plasmas by High Voltage Heavy Ion Beam Probes;* Apr. 1992

NIFS-144 N. Ohyabu, N. Noda, Hantao Ji, H. Akao, K. Akaishi, T. Ono, H. Kaneko, T. Kawamura, Y. Kubota, S. Morimoto. A. Sagara, T. Watanabe, K. Yamazaki and O. Motojima, *Helical Divertor in the Large Helical Device;* May 1992

NIFS-145 K. Ohkubo and K. Matsumoto, *Coupling to the Lower Hybrid Waves with the Multijunction Grill*; May 1992

NIFS-146 K. Itoh, S. -I.Itoh, A. Fukuyama, S. Tsuji and Allan J. Lichtenberg, *A Model of Major Disruption in Tokamaks*; May 1992

NIFS-147 S. Sasaki, S. Takamura, M. Ueda, H. Iguchi, J. Fujita and K. Kadota, *Edge Plasma Density Reconstruction for Fast Monoenergetic Lithium Beam Probing*; May 1992

NIFS-148 N. Nakajima, C. Z. Cheng and M. Okamoto, *High-n Helicity-induced Shear Alfvén Eigenmodes*; May 1992

NIFS-149 A. Ando, Y. Takeiri, O. Kaneko, Y. Oka, M. Wada, and T. Kuroda, *Production of Negative Hydrogen Ions in a Large Multicusp Ion Source with Double-Magnetic Filter Configuration*; May 1992

NIFS-150 N. Nakajima and M. Okamoto, *Effects of Fast Ions and an External*

Inductive Electric Field on the Neoclassical Parallel Flow, Current, and Rotation in General Toroidal Systems; May 1992

NIFS-151 Y. Takeiri, A. Ando, O. Kaneko, Y. Oka and T. Kuroda, *Negative Ion Extraction Characteristics of a Large Negative Ion Source with Double-Magnetic Filter Configuration*; May 1992

NIFS-152 T. Tanabe, N. Noda and H. Nakamura, *Review of High Z Materials for PSI Applications* ; Jun. 1992

NIFS-153 Sergey V. Bazdenkov and T. Sato, *On a Ballistic Method for Double Layer Regeneration in a Vlasov-Poisson Plasma*; Jun. 1992

NIFS-154 J. Todoroki, *On the Lagrangian of the Linearized MHD Equations*; Jun. 1992

NIFS-155 K. Sato, H. Katayama and F. Miyawaki, *Electrostatic Potential in a Collisionless Plasma Flow Along Open Magnetic Field Lines;* Jun. 1992

NIFS-156 O.J.W.F.Kardaun, J.W.P.F.Kardaun, S.-I. Itoh and K. Itoh, *Discriminant Analysis of Plasma Fusion Data*; Jun. 1992

NIFS-157 K. Itoh, S.-I. Itoh, A. Fukuyama and S. Tsuji, *Critical Issues and Experimental Examination on Sawtooth and Disruption Physics*; Jun. 1992

NIFS-158 K. Itoh and S.-I. Itoh, *Transition to H-Mode by Energetic Electrons*; July 1992

NIFS-159 K. Itoh, S.-I. Itoh and A. Fukuyama, *Steady State Tokamak Sustained by Bootstrap Current Without Seed Current*; July 1992

NIFS-160 H. Sanuki, K. Itoh and S.-I. Itoh, *Effects of Nonclassical Ion Losses on Radial Electric Field in CHS Torsatron/Heliotron*; July 1992

NIFS-161 O. Motojima, K. Akaishi, K. Fujii, S. Fujiwaka, S. Imagawa, H. Ji, H. Kaneko, S. Kitagawa, Y. Kubota, K. Matsuoka, T. Mito, S. Morimoto, A. Nishimura, K. Nishimura, N. Noda, I. Ohtake, N. Ohyabu, S. Okamura, A. Sagara, M. Sakamoto, S. Satoh, T. Satow, K. Takahata, H. Tamura, S. Tanahashi, T. Tsuzuki, S. Yamada, H. Yamada, K. Yamazaki, N. Yanagi, H. Yonezu, J. Yamamoto, M. Fujiwara and A. Iiyoshi, *Physics and Engineering Design Studies on Large Helical Device*; Aug. 1992

NIFS-162 V. D. Pustovitov, *Refined Theory of Diamagnetic Effect in Stellarators;* Aug. 1992